Soil Dynamics and Earthquake Engineering 124 (2019) 98–120

Contents lists available at ScienceDirect

Soil Dynamics and Earthquake Engineering

journal homepage: www.elsevier.com/locate/soildyn

Seismic behaviour of rocking bridge pier supported by elastomeric pads on pile foundation

Rajesh R. Rele[a,*], Pradeep Kumar Dammala[b], Subhamoy Bhattacharya[c], Ranjan Balmukund[d], Stergios Mitoulis[e]

[a] Department of Civil and Environmental Engineering, University of Surrey, Guildford, UK
[b] Department of Civil Engineering, Indian Institute of Technology, Guwahati, India
[c] Department of Civil and Environmental Engineering, Faculty of Engineering and Physical Sciences (FEPS), University of Surrey, Guildford, Surrey, GU2 7XH, UK
[d] Principal Consultant (Bridges), R.R Consulting Engineers, Mumbai, India
[e] Department of Civil and Environmental Engineering, Faculty of Engineering and Physical Sciences (FEPS), University of Surrey, Guildford, Surrey, GU2 7XH, UK

ARTICLE INFO

Keywords:
Bridges
Pier
Rocking isolation
Elastomeric pad
Resilient

ABSTRACT

Life line structures such as elevated flyovers and rail over bridges should remain functional after an earthquake event to avoid possible traffic delays and risk to general public. Generally, restraining the structure by reducing the degrees of freedom often cause serious damages that occurs during a seismic event through yielding of the structural components. By allowing the structure to rock through uplift using suitable arrangements can be a plausible seismic resilient technique. In this context, this article proposes a novel seismic resilient pile supported bridge pier foundation, which uses elastomeric pads installed at top of pile cap. The effect of pile soil interaction along with ground response analysis is also incorporated in the full bridge model adopted for the study. One dimensional equivalent linear site response analyses were performed to arrive at the amplified/attenuated ground motions along the depth of soil.The seismic performance of the proposed bridge with new rocking isolation concept is compared with existing bridge located in medium seismic zone of India. With the help of non-linear dynamic time history analysis and nonlinear static pushover analysis, the bridge modelled using the proposed novel rocking isolation technique shows good re-centering capability during earthquakes with negligible residual drifts and uniform distribution of ductility demand along the piers of the bridge considered in this study.

1. Introduction

Bridges and flyovers are major assets of any country and failure of such structures during seismic event leads to economic loss to the country and traffic disruptions to the general public. Despite their importance, these key infrastructure assets have been designed for many years, neglecting the fact that loads and geo-hazards may change drastically and thus significant upgrades may be required during their service life. Societies expect accelerated constructions, minimal damage and rapid upgrading for bridges which are sources of transportation and thus must be designed to face very strong earthquake in order to avoid permanent drift which are beyond repairs. Collapse of whole bridge caused by extended damage of the piers and/or unseating of the superstructure caused by insufficient deformation capacity of the bearing and other destruction of bridge structure often occurs in an earthquake [1].The concept of ductility is used in the conventional design of bridge pier wherein the pier reinforcement is detailed to develop flexural plastic hinges at the base and top of pier [2]. Although bridges designed in this manner may undergo damages due to severe earthquake excitations as observed in Fig. 1(a)–(d). Rocking isolation in the form of structural rocking or geotechnical rocking of the bridge pier experience far less damage when subjected to high intensity earthquake ground motion with added bonus of pier that recenter due to the increased period of vibration owing to the flexibility of the resilient pier [3,4]. The design of South Rangitikei Railway Bridge in New Zealand in 1981 used structural rocking by adopting the concept of dissipative rocking at the pier-to-foundation interface by means of prestressing tendons which had more rocking sections contributing to dissipation of energy and thus less prone to heavy damages when subjected to severe earthquakes [5,6]. Antonellis et al [7] investigated the three dimensional seismic response of conventional fixed based pier and piers rocking on pile

* Corresponding author.
E-mail addresses: r.rele@surrey.ac.uk (R.R. Rele), pradeepkumardammala@gmail.com (P.K. Dammala), s.bhattacharya@surrey.ac.uk (S. Bhattacharya), rbalmukund@rediffmail.com (R. Balmukund), s.mitoulis@surrey.ac.uk (S. Mitoulis).

https://doi.org/10.1016/j.soildyn.2019.05.018
Received 22 December 2018; Received in revised form 4 April 2019; Accepted 12 May 2019
Available online 30 May 2019
0267-7261/

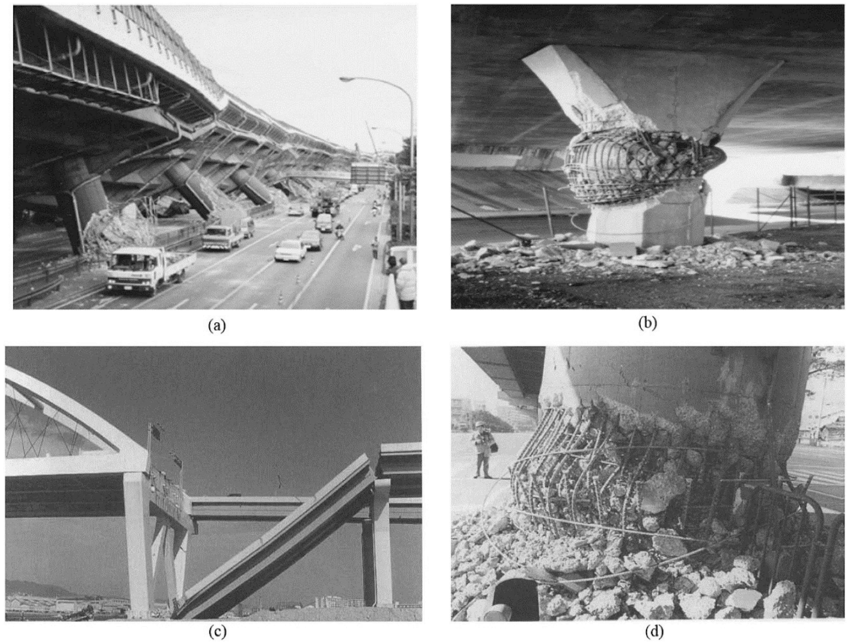

Fig. 1. (a) Collapse of Hanshin expressway 1995 Kobe earthquake (b) Column failure in 1994 Northridge earthquake (c) Unseating of simply supported link span in 1995 Kobe earthquake (d) Bridge pier failure in Loma Prieta earthquake in 1989.

foundations that are designed to remain elastic. The rocking of pile foundation was achieved by wrapping the protruding part of piles into the pile cap by neoprene sheet and rubber pad. Experimental investigation of rocking pile group foundation has also been studied by Guan et al [31]. They used rubber pad and foam strip at the junction of pile and pile cap to allow uplift and rocking of pile cap. This new rocking model proposed by them showed excellent seismic resilience with reduced residual drifts at the top of bridge pier.

Jacquelyn et al [8] identified many unique features of rocking on unattached piles and demonstrated that it is viable design concept. The scope included detailed description of the new design mechanism raised by rocking foundation on unattached piles which may not be faced in traditional foundation design. Silva et al [9] studied the rocking of pile caps over the piles by considering the piles not vertically anchored to the pile cap.

Agalianos et al [12] proposed two rocking isolation techniques. The first one allows the pier to rock on the foundation while the piers are not monolithically connected to the foundation but are designed to uplift and rock under seismic motion. They suggested a recess shall be provided in footing to avoid sliding of pier and promote only rocking phenomenon. The second concept promotes rocking of the pier and foundation assembly by full mobilization of the soil bearing capacity.

This paper proposes application of a rocking resilient bridge pier foundation which uses elastomeric pad incorporated beneath the footing of bridge piers with pile foundation. The main aim of this paper is to evaluate the seismic resilience (only in longitudinal direction of bridge) of the conventional system (Fig. 2(a)) and the proposed rocking system (Fig. 2(b)). The conventional system adopted is an existing Rail Over Bridge (ROB) located in Vishakapatam, India. The paper is structured in the following way: First, the existing bridge is described along with its structural details. The proposed bridge with new rocking isolation technique is then mentioned. This is followed by detailed description of the finite element model created for the both the bridges in this study along with the effect of soil pile interaction and ground response analysis.

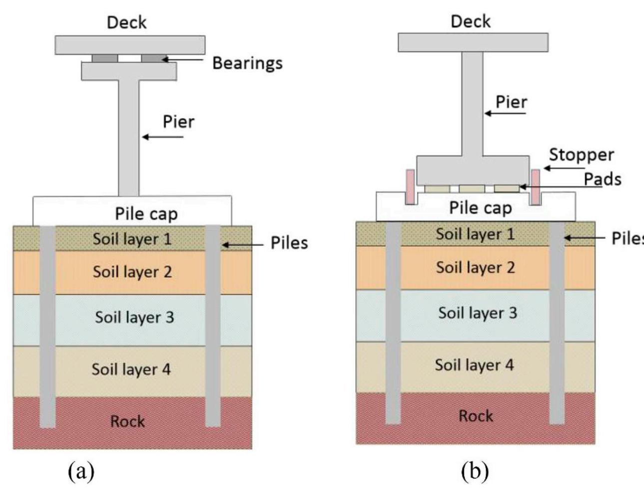

Fig. 2. Studied configurations (a) Conventional system (b) Proposed rocking system.

2. Description of bridge models

2.1. Conventional system

An existing rail over bridge (ROB) located in Visakhapatnam city of Andhra Pradesh in India is considered as case study, forming the basis for the developed numerical models. A numerical model of the ROB is developed as per the actual soil conditions and restraints in the structure. The existing bridge is four span simply supported prestressed concrete box girder with width of 19.75 m and length of 133 m. The spans are of variable lengths due to the rail lines found below the bridge as shown in Fig. 3(a). The height of pier for all the span is uniform and is 7.7 m. The pier (as shown in Fig. 3(b)) rests on pile cap with pile of 1 m diameter with different pile configuration as per the actual design made based on geotechnical investigation. The abutment pier as shown

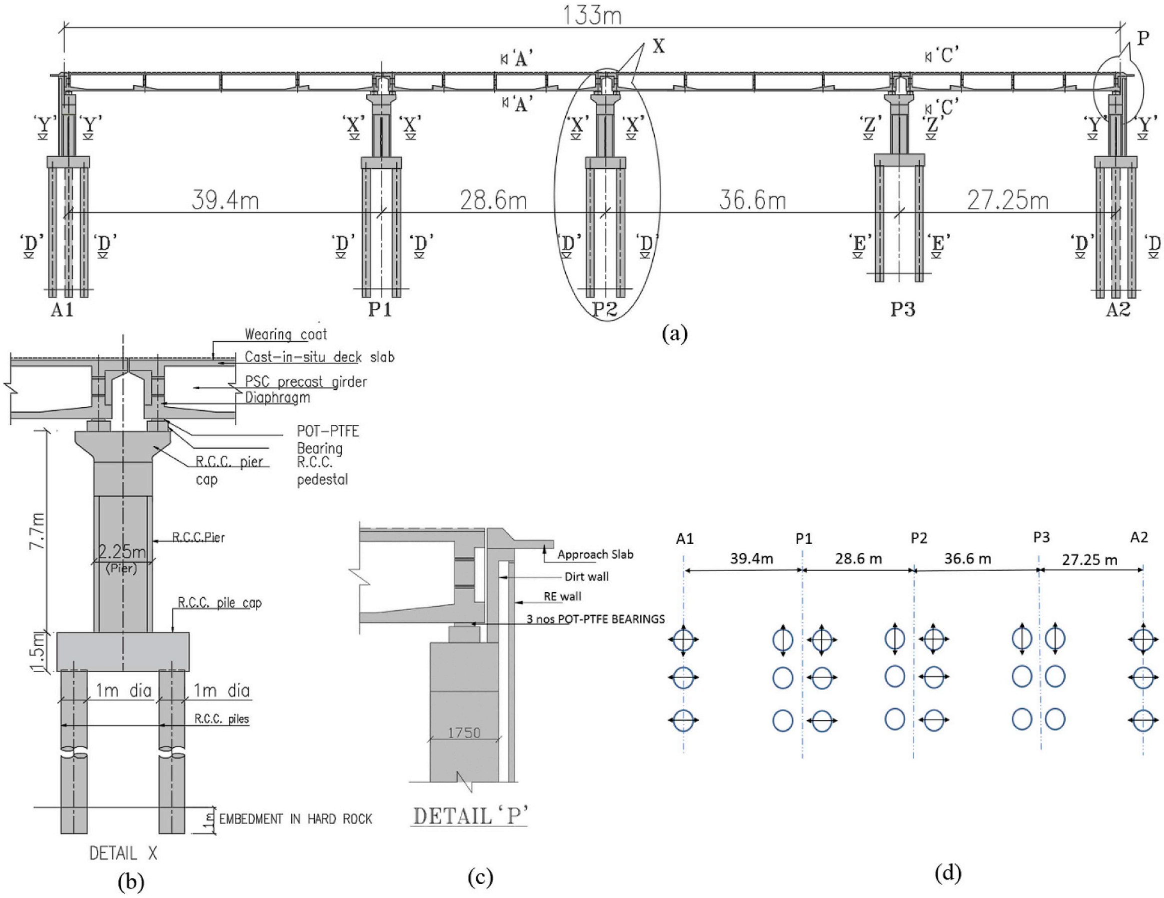

Fig. 3. Existing Rail over Bridge in Visakhapatnam, India (a) Elevation (b) Pier details (c) Detail P at abutment piers A1 & A2 for both the bridges considered in the study (d) Disposition of bearings along span.

in Fig. 3(c) has been separated from soil by means of reinforced earth (RE) wall and thus all soil pressure is exerted only on RE wall while abutment pier is free from any lateral pressure of soil. The superstructure rests on pier cap on POT-PTFE (Poly Terta Fluro Ethylene) bearings as per the disposition shown in Fig. 3(d). The superstructure of the ROB consists of box girder section as shown in appendix. The ROB is designed according to provision of Indian Road Congress (IRC) codes [13,14,15].

2.2. Proposed bridge pier rocking on elastomeric pads

An alternative proposal to the existing bridge considered in this study is shown in Fig. 4(a). In this proposal, the intermediate piers and abutment piers along with its footing rocks on elastomeric pads which are placed on top of pile cap as shown in Fig. 4(a),(b) and (c). The recess made in the pile cap are for stoppers to restrict horizontal sliding and thus allow only rocking of the bridge pier without any translational movements to avoid any walking off phenomenon [3]. In practice, a thin cushion in the form of rubber pad is attached vertically alongside of the stopper in order to avoid damage to footing due to pounding of the two concrete surfaces. For future replacement of bearings, jack locations are shown in Fig. 4(d). The diameter of flat jack [16] shall be 350 mm in the transverse direction of bridge having load carrying capacity of 1100 kN and 450 mm in longitudinal direction having load carrying capacity of 1700 kN to lift the system by 6–10 mm so that pads can be replaced. The pads in the center of footing are replaced first after the stoppers and pads at periphery are removed. The material and geometry of pier and piles are kept the same as per the existing bridge for comparative study. The superstructure (Fig. 4(e)) is monlothic (integral) at all the pier location including those at abutment ends.

2.2.1. Material and geometry of pier and piles

The existing bridge has three intermediate piers (P1, P2 and P3) and two abutment piers (A1and A2) with rectangular cross-section as shown in appendix.

The material of piers and the reinforcing steel ratio ρ_l, conforming to IRC 112 [15] is shown in Table 1 while for piles is shown in Table 2. The abutment piers (A1& A2) has five piles while P1 and P2 piers have six piles. The pier P3 have eight piles as per the actual design and strata of the soil encountered at the site. The pile configuration and reinforcement details of all the piles are shown in Appendix.

3. Numerical modelling of full bridge models

The proposed rocking bridge and the existing bridge are modelled in *CSi Bridge* [17] as shown in Fig. 5 and Fig. 6 respectively. The pile soil interaction is considered as per the actual site scenario and the displacement time histories that are obtained from independent free field site response analysis are applied to pile nodes in the form of multi-support excitation. A nonlinear stage construction case for proposed rocking bridge is defined in which elastomeric pads are deformed first due to self-weight of pier, footing and dead load of the superstructure. The nonlinear time history analysis was performed using the stiffness at end of this nonlinear stage construction case. The superstructure was modelled using frame elements as per the cross-section of the existing bridge. The dead load mass of the superstructure and the superimposed dead load due to crash barrier, footpath slab and wearing coat was activated during the construction stage analysis performed in the computer programme.

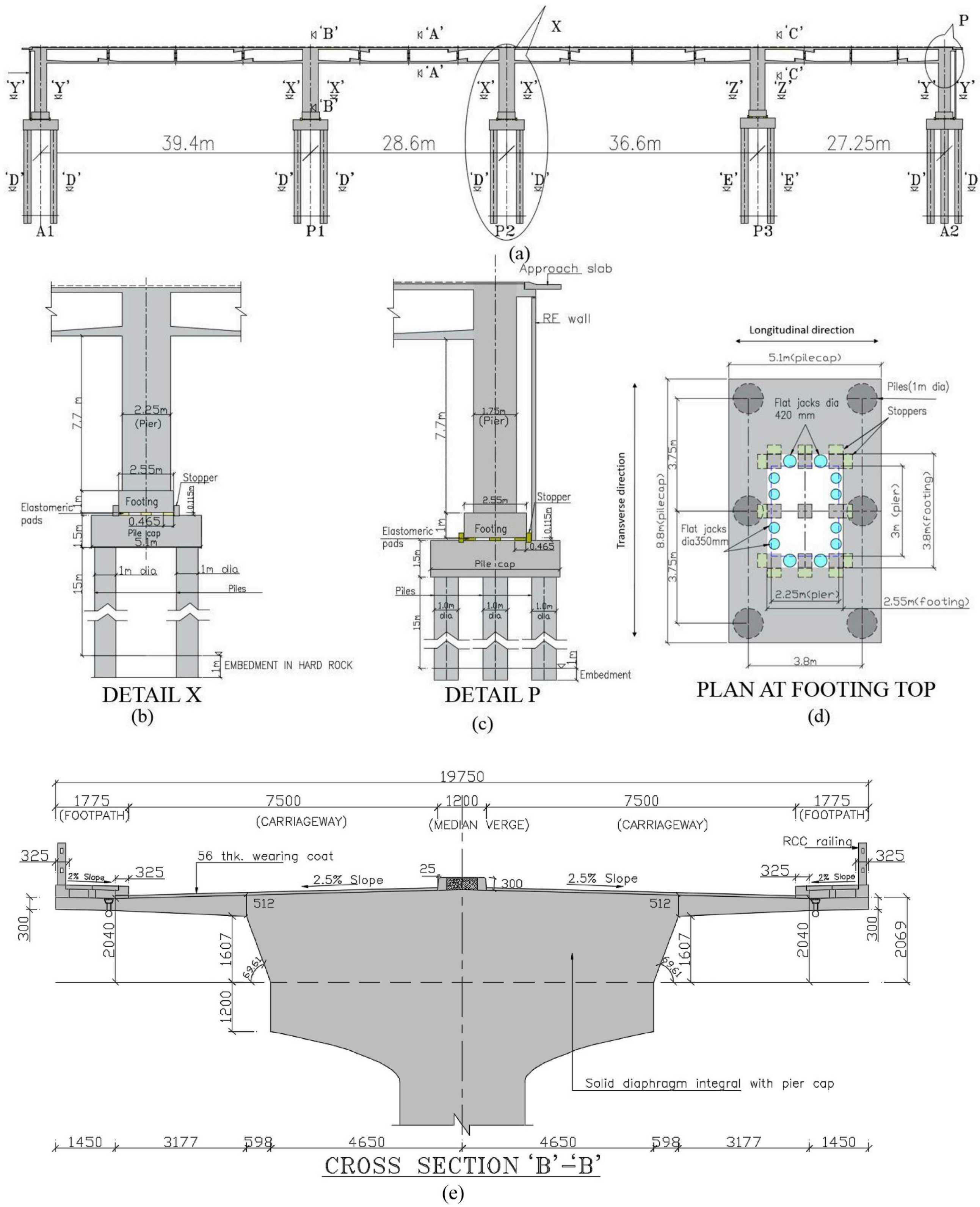

Fig. 4. Proposed rocking bridge (a) Elevation (b) Rocking Pier details at pier end (c) Rocking Pier details at abutment pier (d) Top plan of footing of rocking piers (e) Superstructure section integral with pier.

3.1. Nonlinear modelling of piers and piles

To stimulate post-yield behaviour of piers, a concentrated plastic hinge is assigned to the frame element of the pier. Deformation beyond the elastic limit occurs only within the hinges modelled at the top and the bottom of pier for rocking pier, while the hinge is assigned only at bottom for conventional pier because negligible bending moments are expected at the pier top in this case. Similarly, for pile the hinge is assigned at top of pile below the pile cap. Inelastic behaviour is obtained through integration of the plastic strain and plastic curvature

Table 1
Material properties for pile.

Pile	Grade of Concrete	ρ_l = As/Ac (%)
A1 (5nos)	M-35	1.56
P1(6nos)	M-35	1.56
P2(6nos)	M-35	1.56
P3(8nos)	M-35	2.15
A2(5nos)	M-35	1.56

Table 2
Material Properties for pier.

Pier	Grade of Concrete	ρ_l = As/Ac (%)
A1	M-35	0.4
P1	M-35	0.52
P2	M-35	0.52
P3	M-35	1
A2	M-35	0.4

which occurs within the pre-defined hinge length. To capture the coupled axial and bending behaviour, P-M3 hinge is assigned to the piers and piles at relevant locations with the input hinge model being the moment-curvature graph which is shown in Fig. 7(a) for pier P1 and Fig. 7 (b) for pile P1 only. The moment capacity of piles and pier for axial load due to dead load of superstructure is shown in Tables 3 and 4 respectively. The hinge length for pier is of 0.850 m and for pile is 1.475 m which are calculated as per the equation given by Priestley [2]. The idealized moment-curvature graph is obtained by balancing the areas between the actual and the idealized M-φ (where φ is the curvature) curves beyond the first reinforcing bar yield point as per Caltrans seismic design criteria [18]. The confinement of reinforced concrete sections has been taken into account using the Mander [19] confined model to represent the stress-strain behaviour of the concrete core. The type and number of elements used for each bridge model is shown in Tables 5 and 6. The numerical model details of the rocking bridge and the existing bridge in both the directions are shown in Figs. 8–11 along with displacement time history applied at end soil spring element only in longitudinal direction of the bridge.

3.2. Elastomeric pads supporting the pier footing

A total of 9 pads (Fig. 4(d)) are modelled using friction isolators available in the chosen computer programme [17].The friction isolators has coupled friction properties for shear deformations and carries only compression. This particular non-linear link element was chosen since the footing simply rests on bearings and thus compression is only allowed in the link element while friction between pad and footing is modelled by setting coefficient of friction as 0.8. The friction isolator model is based on hysteretic behaviour proposed by Wen [20] and recommended for base isolation by Nagarajaiah [21]. The size of bearing is 465 mm × 465 mm with height of 115 mm which consists of three rubber layers of 35 mm thickness and two steel shims of 5 mm thickness was selected after the design of pad was made as per Eurocode [22]. This particular size of bearing was chosen to avoid any large uplift of footing and also to control large vertical initial compression of pad.

The vertical (k_v) and horizontal stiffness (k_h) of bearing is evaluated using following equations [23]:

$$k_v = \frac{E_c A}{\sum t_i}\pi; \tag{1}$$

$$k_h = \frac{G\,A}{\sum t_i}; \tag{2}$$

$$E_c = \frac{Ec'B}{Ec' + B}; \tag{3}$$

$$E_c' = 6.73\,GS^2 \tag{4}$$

where, ***G*** is the shear modulus of the bearing having value of 0.7 MPa, ***B*** is the bulk modulus as 2000 MPa and ***S*** is the shape factor which for square pad is ***a***/4***t*** where "***a***" is size of rubber pad and t is the thickness of each pad. The initial vertical deformation of pad with superstructure load is found to be 15.5 mm and the stress in pad is found to be 6.56 MPa against permissible stress of 10–25 MPa as per Eurocode [22].

For the existing bridge model, the Pot –PTFE bearings are modelled as per the degree of freedom rather than stiffness. The behaviour of such bearings are dependent on their direction of movement rather than stiffness which are quite high since the deformation of these bearings are only 3–4 mm resulting in rigid behaviour due to top steel plate anchored in the superstructure.

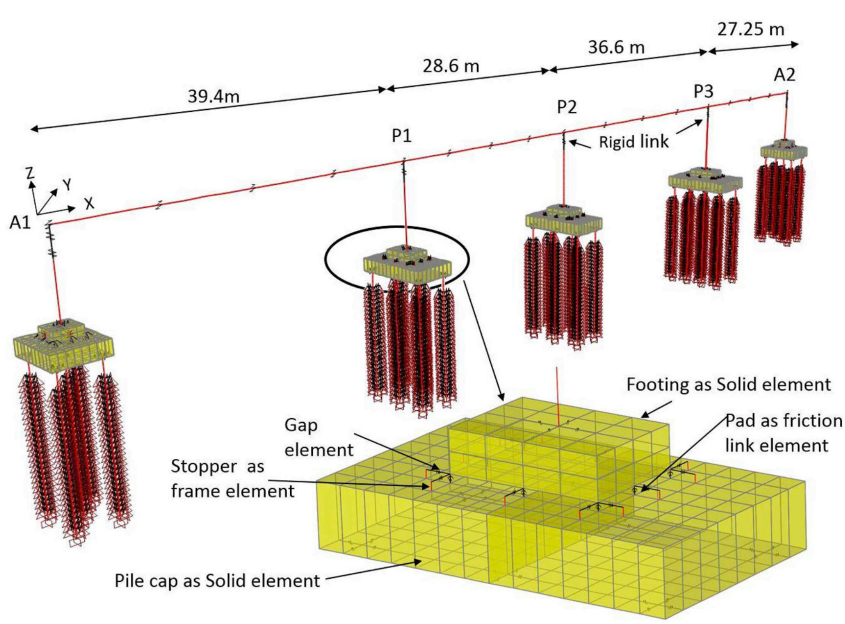

Fig. 5. Finite element model of proposed rocking bridge.

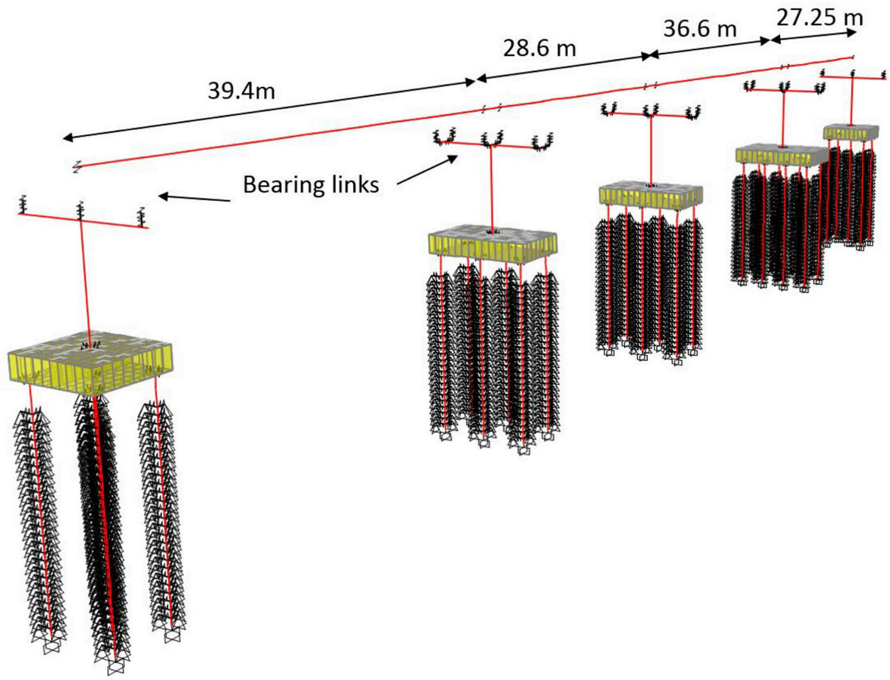

Fig. 6. Finite element model of existing bridge.

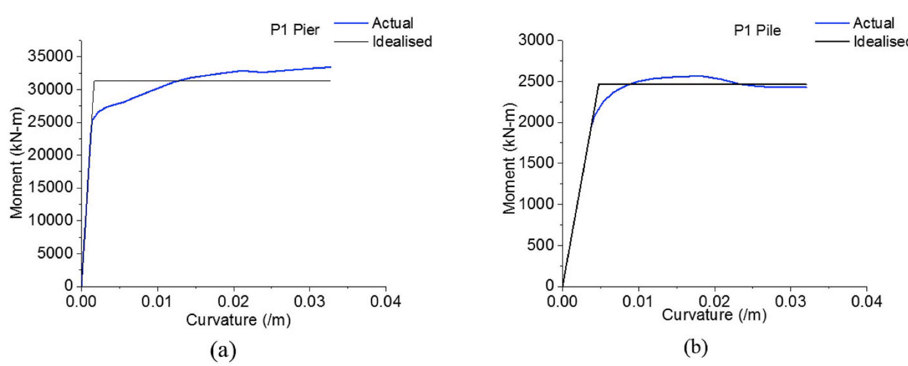

Fig. 7. Moment-curvature relationship for (a) Pier P1 with 0.52 %steel (b) Pile P1 with 1.56%steel.

Table 3
Moment capacity of piles.

Pile	Axial load P(kN)	Yield Moment My (kN.m)	Ultimate Moment Mu (kN.m)
A1	1400	1770	2450
P1	2140	1980	2600
P2	1900	1900	2540
P3	1500	2210	2940
A2	1100	1700	2350

Table 4
Moment capacity of Pier.

Pile	Axial load P(kN)	Yield Moment My (kN.m)	Ultimate Moment Mu (kN.m)
A1	6150	9320	14440
P1	12470	23590	34550
P2	10620	21910	33350
P3	11230	35220	50720
A2	4530	8320	13510

4. Pile soil interaction

The pile soil interaction is modelled by using nonlinear discrete Wrinkler springs as adopted by Quinn [10]. Boulanger et al [11]. The soil profile on which all the piles of the existing bridge are found is as shown in Table 7. The pile are anchored to depth of 1.5 times the diameter in hard rock found at site location of Vishakhapatnam where the ROB was constructed. To simulate lateral soil resistance(p-y springs) and vertical soil resistance (friction-*t*-z springs) along piles, nonlinear springs were attached at 0.5 m interval for a 15 m long pile. The typical force-deformation (p-y and t-z) curves which are obtained from equations (5) and (6) respectively are only shown for soft clay at 6 m depth and hard clay at 10 m depth in Fig. 12 and Fig. 13 as per the API [24]method.

$$p_u = 3c + \gamma X + J\frac{cX}{D} \tag{5}$$

$$f = \alpha .\ c \tag{6}$$

$$\alpha = 0.5\psi^{-0.5} \qquad \psi = {}^{c}/_{p'} \leq 1$$

$$\alpha = 0.5\psi^{-0.25} \qquad \psi = {}^{c}/_{p'} > 1$$

Table 5
Elements used in proposed rocking bridge.

Component	Type of element	No. of elements
Superstructure	Frame	131
Pier	Frame	10
Footing of Pier	Solid	32
Pile Cap	Solid	270
Piles	Frame	15

Table 6
Elements used in of existing bridge.

Component	Type of element	No. of elements
Superstructure	Frame	131
Pier Cap	Frame	10
Pier	Frame	10
Pile Cap	Solid	270
Piles	Frame	15

where pu = ultimate resistance, kPa.

c = undrained shear strength of clay;
X = soil depth from top of soil layer to specified node;
J = dimensionless constant as 0.5
D = Diameter of pile section.
p' = effective overburden pressure at the point of consideration.

5. Selection of earthquake excitations

The fixed pier pile foundation and resilient pier pile foundation were analysed for seven real accelerograms compatible to ground Type 1- C-dependent Eurocode elastic spectra based on the recommendations of the Eurocode [25]. The Peak Ground Accelerations (PGA) selected was 0.3 g which is the average of the two maximum seismic zones of India where the existing bridge is located. The response spectra and the analysed accelerograms are shown in Fig. 14 and Fig. 15 respectively.The seismic motion is applied only in the longitudinal direction of the bridge. The characteristics of the earthquake records considered in the study is shown in Table 8.

5.1. Free field ground response analysis

In order to obtain the variation of PGA over the depth, 1D equivalent linear site response analysis has been performed using a computer program (DEEPSOIL [26]) as shown in Fig. 16. This program requires the user to input the soil properties along with the chosen input acceleration time histories in order to provide the varying ground motion histories along the depth of the profile. Similar equivalent analysis has been performed for a bridge site in Northeast India [29] using DEEPSOIL program.

A hard rock with a SPT N value > 100 was observed in the borehole data at the bottom of the profile and hence, the chosen motions are applied considering a rigid bedrock base. The variation of PGA and peak displacement along the depth can be observed in Fig. 17 (a) and Fig. 17 (b) where a significant amplification of the input waves can be noted. Such amplification can be justified by the induced high strains in the soil column and reduced shear strength [30].The obtained acceleration time histories are then converted to displacement time histories which are applied at each pile soil spring node in the developed finite element model. Only excitation in longitudinal direction of the bridge is considered in this study.

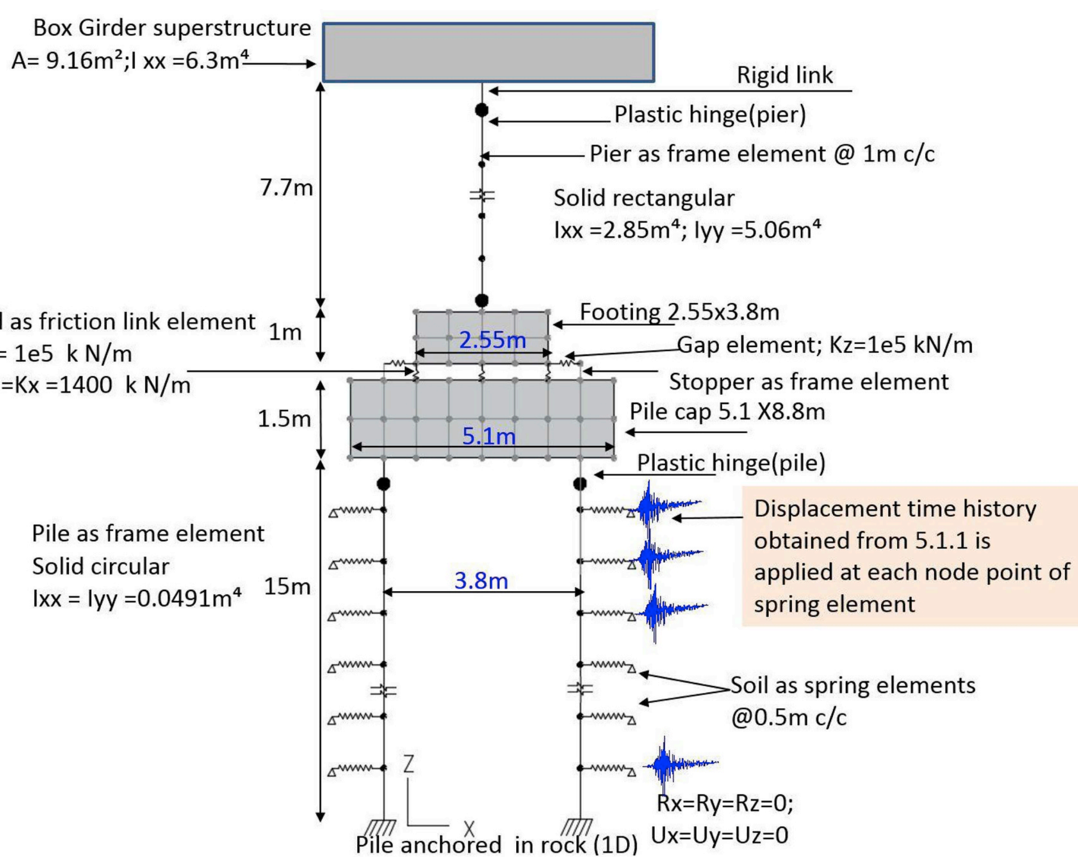

Fig. 8. Numerical model details in longitudinal direction of bridge of rocking bridge pier foundation on elastomeric pads.

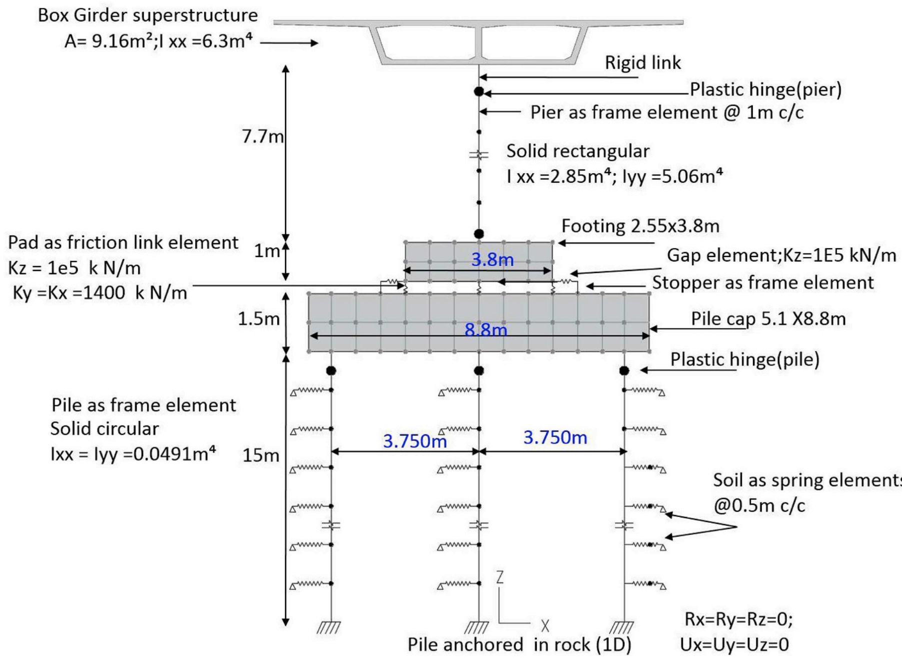

Fig. 9. Numerical model details in transverse direction of bridge of rocking bridge pier foundation on elastomeric pads.

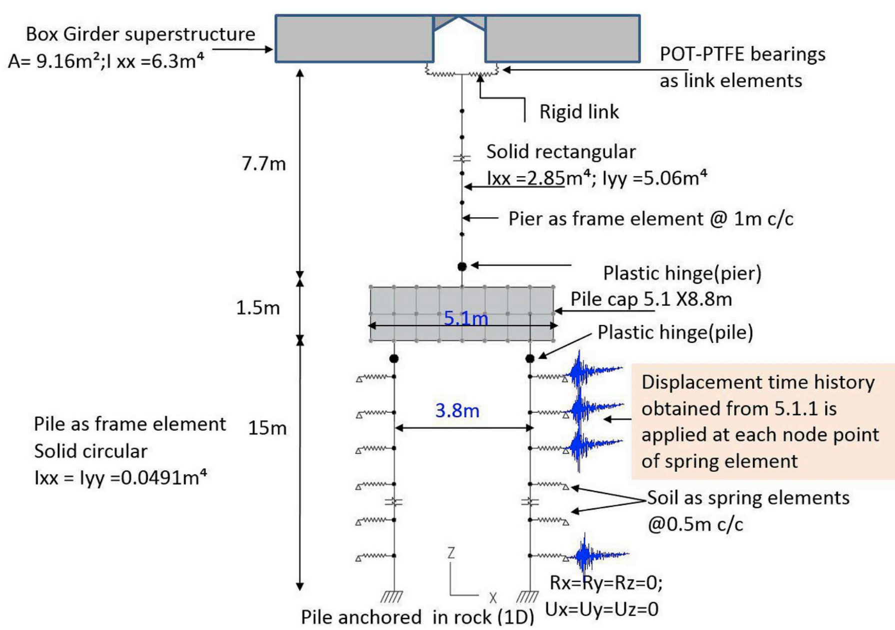

Fig. 10. Numerical model details in longitudinal direction of bridge of conventional bridge pier foundation.

6. Results and discussion

The effective fundamental period for proposed rocking bridge was 1.42 s while for existing rail over bridge was 1.01 s. The increase in fundamental period of vibration is found to be 40% since the elastomeric pads provided beneath the pier footing enhanced the flexibility to the rocking bridge system.

The first three modes of both bridges are shown in Fig. 18 and Fig. 19. The modal participating mass ratio is 0.679 for the first mode which is in transverse direction for the proposed rocking bridge while is 0.716 bridge in the longitudinal direction for the existing bridge. The modal analysis helps to identify the weak direction of the structure and the modes with relatively high effective mass can be easily activated by base exciation.

The comparison of responses for all the five piers of both the bridges are shown in Fig. 20 to Fig. 23 for Imperial seismic event having PGA of 0.3 g. The Tables 9 and 10 shows the mean values of responses of pier and piles, which are calculated based on the seven acceleration time histories for PGA of 0.3 g for the existing bridge and the proposed rocking bridge.

6.1. Comparison of bending moments in pier and piles

It can be seen from Tables 9 and 10 that bending moment of piers in rocking bridge are reduced approximately by 77% and 60% for piers P2 and P3 respectively as compared to the conventional existing bridge. The pier P1 of the rocking bridge showed lesser variation as it is supported by large span and is close to the rocking abutment pier as well.

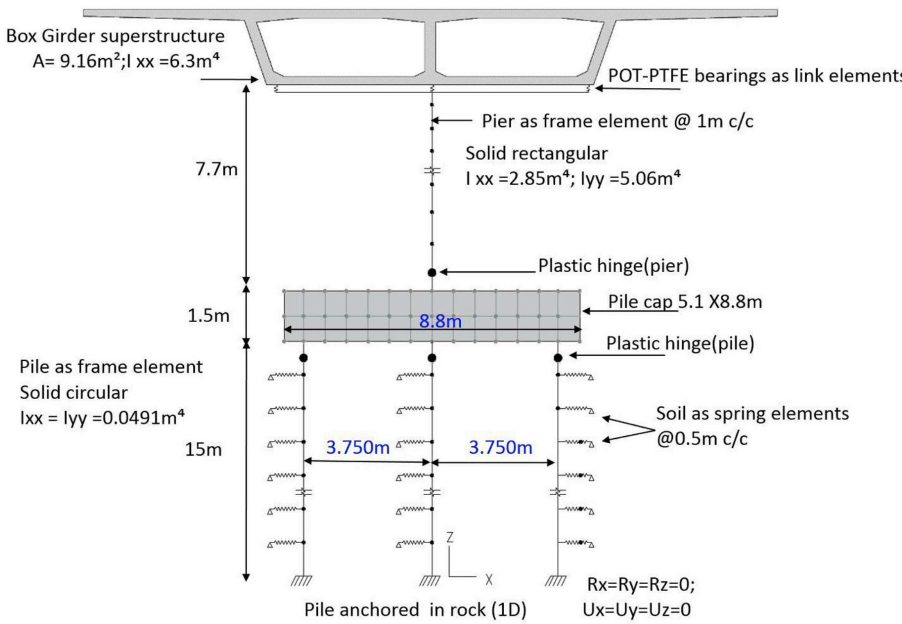

Fig. 11. Numerical model details in transverse direction of bridge of conventional bridge pier foundation.

Table 7
Soil profile at all pile locations.

Soil type	Depth, m	SPT,N	Vs, m/s	ϒ total, kN/m^3
Filled Soil	0–3.5	6	178.5	18
Sandy Clay	3.5–6	7	190.7	19.6
Soft Clay	6–8.5	5	165	18
Hard Clay	8.5–12.5	12	240	20.41
Soft Rock	12.5–15	36	385	22
Hard Rock	15–18	100	598	26

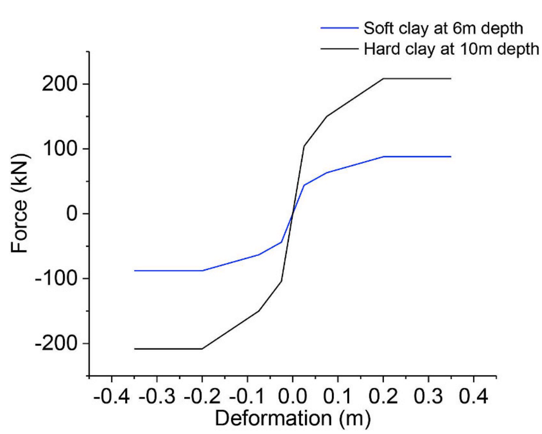

Fig. 12. Typical Force deformation curve for pile soil spring for soft clay (at 6 m depth) and hard clay (at 10 m depth).

The pier moments in the existing bridges are high as expected since the pier acts as cantilever structure having the superstructure disconnected by means of bearing provided at the pier top. For the proposed rocking bridge, the bending moment in the piers are reduced due to its integral superstructure (including at the abutment ends) and the footing which rocks on elastomeric pads provided at the base of pier. The abutment piers of the rocking bridge also showed reduced bending moment of 13% and 28% at pier A1 and A2 respectively as compared to existing bridge. For both the bridges, pier remain elastic as the bending moment did not exceed the yield moments. The bending moment in piles of rocking bridge were decreased by 12.5%, 4.3%, 25% 7.5% and 14.6%

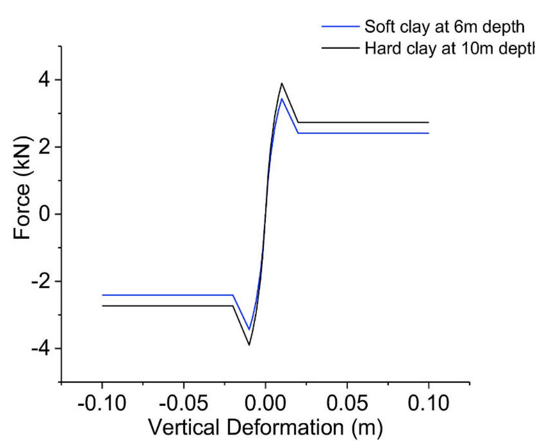

Fig. 13. Typical Force deformation curve for axial soil pile interaction for soft clay (at 6 m depth) and hard clay (at 10 m depth).

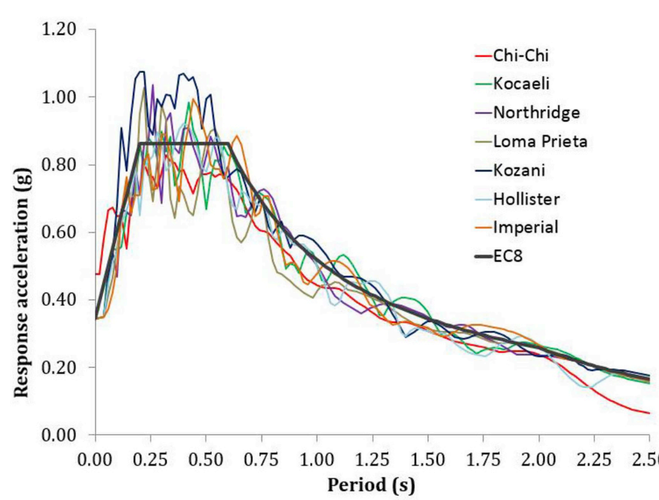

Fig. 14. Response spectra of accelerograms compatible to ground Type C-dependent Euro code 8–1 elastic spectra (PGA = 0.30 g).

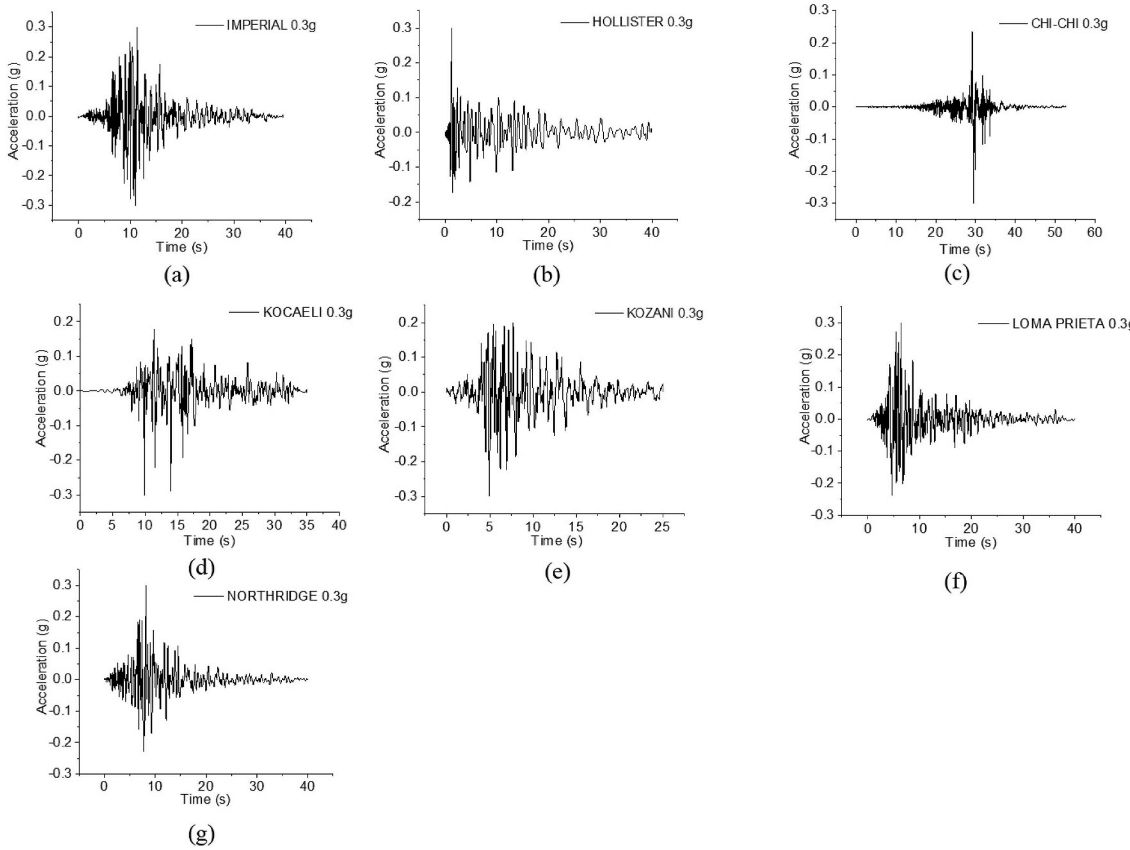

Fig. 15. Acceleration time histories matched to ground Type C-dependent Euro code 8–1 elastic spectra for 0.3 g (a) Imperial (b) Hollister (c) Chi-chi(d) Kocaeli (e) Kozani (f)Loma Prieta (g) Northridge.

Table 8
Characteristics of selected earthquake records.

Earthquake	Event Year	Station	Magnitude	Duration (s)	Rrup (kM)	Fault type	Soil Type
Hollister	1988	Hollister array 3	5.45	39.89	13.11	Strike slip	Rock
Imperial	1979	Imperial valley	6.54	39.46	23.85	Strike slip	Rock
Kocaeli	1999	Aydin	7.51	34.94	349.45	Strike slip	Rock
Kozani	1995	Kardista	6.4	25	79.3	Normal	Rock
Chi-Chi	1999	CHY002	7.6	52	24.96	Reverse Oblique	Rock
Loma Prieta	1989	Apeel 10-Skyline	6.93	39.89	41.88	Reverse Oblique	Rock
Northridge	1994	Northridge-17645 Saticoy	5.28	39.86	11.14	Reverse	Rock

Rrup = Closest distance to fault rupture.

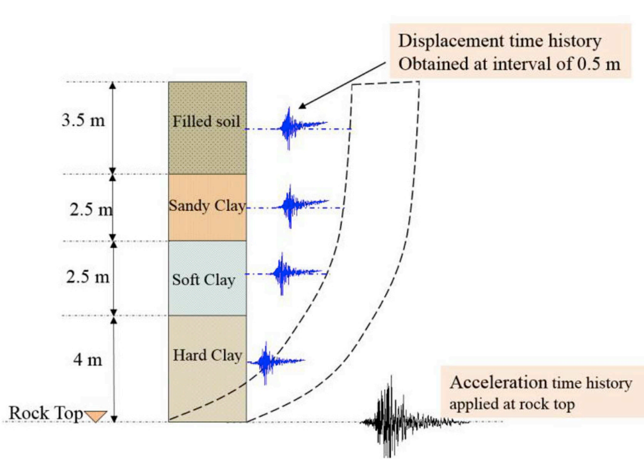

Fig. 16. Free field ground resonse analysis of the soil profile at existing bridge.

for piers A1, P1, P2, P3 and A2 respectively as compared to the rail over bridge considered in this study. The reasoning for this is that the rocking bridge has complete frame action in the longitudinal direction as well as rocking footing making the system subjected to lesser forces and moments. The time history comparison of bending moment in the pier is shown in Fig. 20 for Imperial earthquake only.

6.2. *Comparison of axial forces in pier and piles*

It is observed that the rocking bridge piers and the conventional bridge piers showed negligible axial load fluctuations. Also,in the rocking bridge, pier is not subjected to any tension and hence uplift of superstructure is not a concern for the proposed new system of bridge piers. The time history comparison of axial force in the pier is shown in Fig. 21 for Imperial earthquake only.

6.3. *Comparison of shear forces in pier and piles*

The abutment piers of the rocking bridge are subjected more shear

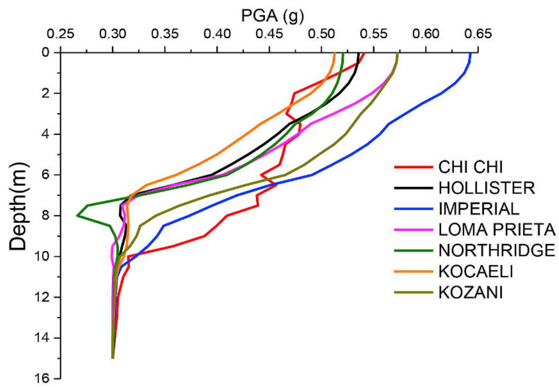

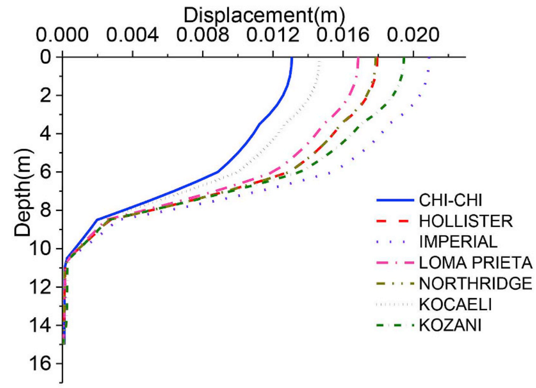

Fig. 17. (a) Amplification of PGA for all the seven earthquakes (b) Amplification of relative displacement for all the seven earthquakes.

forces than the conventional one. Thus, it shall require closer spacing of stirrups and ties than the fixed based system of pier considered in this study. The ratio of shear forces of rocking piers to the conventional piers for A1, P1, P2, P3 & A2 are 1.18,1.84,0.34,0.63 & 1.25. Since the pier P2 being central one it is subjected to less shear force than other piers as observed in both the bridges considered in this study. The shear force in the pier piles of the rocking bridge is reduced by 60% while those in abutment piles are reduced by nearly 20%. The time history comparison of shear force in the pier is shown in Fig. 22 for Imperial earthquake only.

6.4. Comparison of pier (Ux) displacements

The pier horizontal displacements (Ux) of the rocking bridge are reduced considerably than that of the conventional bridge as seen in Tables 9 and 10. This can be explained by the fact that the rocking bridge has integral superstructure with all the piers and thus a complete frame action is available in the longitudinal direction. Furthermore, the configuration of stiff elastomeric pads and stoppers which also controls the uplift of footing placed beneath the pier also plays a vital role in controlling the pier displacments. The time history comparison of axial force in the pier is shown in Fig. 23 for Imperial earthquake only.

6.5. Comparison of residual and maximum drifts

The Tables 11–14 shows the drift comparison for the two bridges considered in this study. The rocking bridge piers showed almost full recentering capacity and did not experience any high permanent drift when subjected to PGA of 0.3 g as seen in Table 12. The existing rail over bridge showed residual drift of 0.103% at pier P1 of the existing bridge as compared to residual drift of 0.021% at pier P1 of the rocking bridge.The abutment piers of the rocking bridge are subjected to less maximum drift than the conventional one as the abutment ends are also integral with the superstructure. The Fig. 24(a) and Fig. 24(b) shows comparison of residual drift and maximum drifts along span of the bridges at the pier locations.

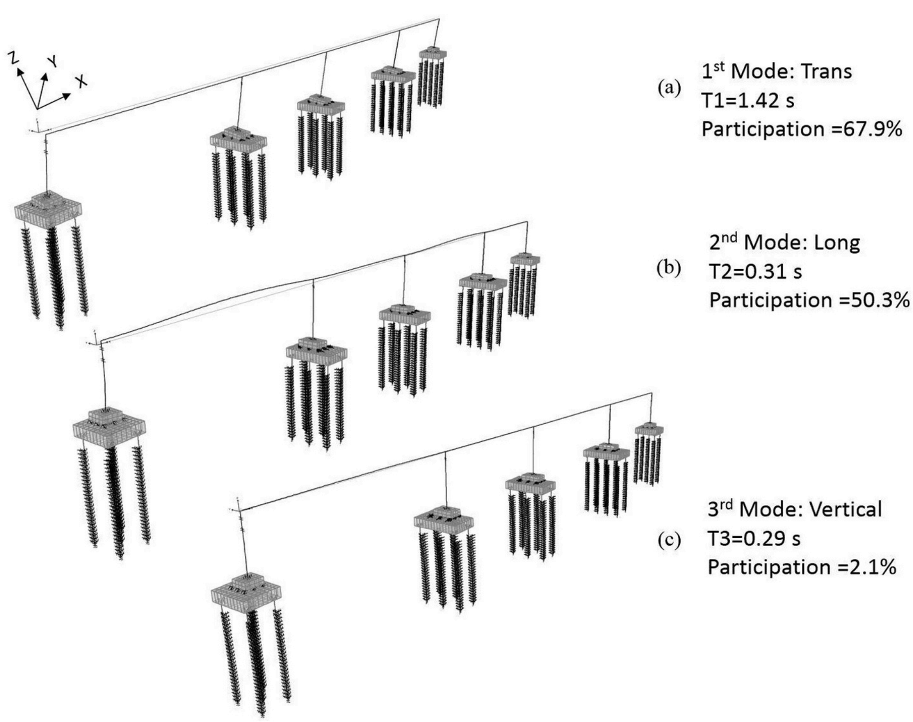

Fig. 18. Modes shapes of rocking bridge (a) First mode (T = 1.42s) (b) Second mode (T = 0.31s) (c) Third mode (T = 0.29 s).

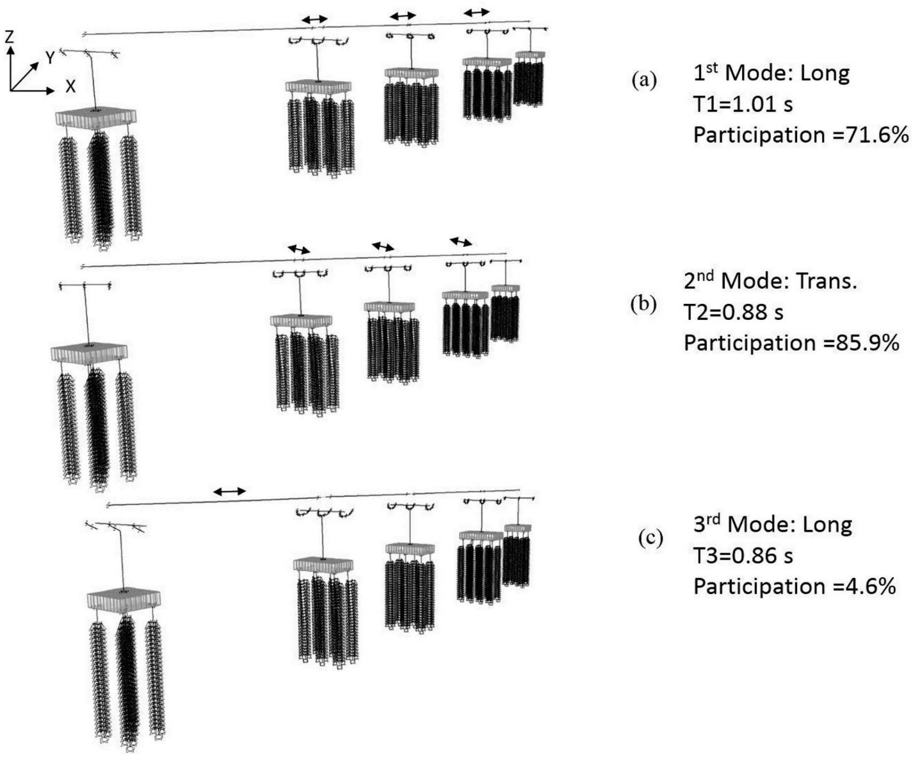

Fig. 19. Modes shapes of existing bridge (a) First mode (T = 1.01s) (b) Second mode (T = 0.88 s) (c) Third mode (T = 0.86s).

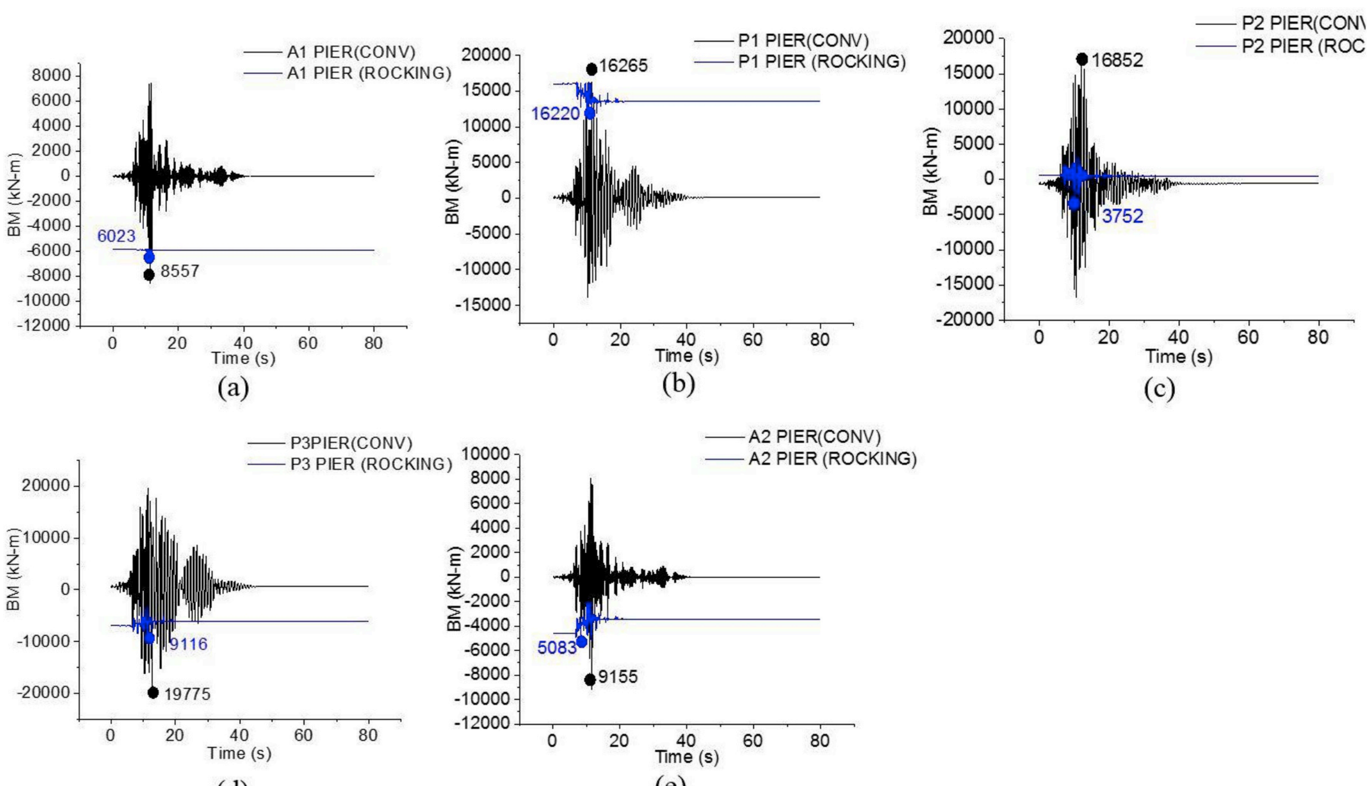

Fig. 20. Time history comparison of Pier bending moment for conventional bridge and the proposed rocking bridge for Imperial earthquake of PGA 0.6 g (a) Pier A1 (b) Pier P1 (c) Pier P2 (d) Pier P3 (e) Pier A2.

Table 9
Average of the maximum values of the seismic loading for PGA 0.30 g (Existing Bridge).

Parameter	PGA 0.3 g (Existing Bridge)				
	Pier A1	Pier P1	Pier P2	Pier P3	Pier A2
Horizontal movement at pier top (mm)	39	17.7	19.5	19	42
Residual Drift (%)	0.063	0.102	0.044	0.093	0.05
Axial force (kN) in pier (max/min)	−7536/-6605	−12457/-11427	−11702/-11006	−11741/-11016	−5566/-5037
Axial force (kN) in piles (max/min)	−3577/-252	−3850/-890	−4360/-630	−4140/10.5	−3330/170
Shear force (kN) in pier	1160	2050	1990	2790	1200
Shear force (kN) in piles	510	300	340	290	530
B.M (kN.m) in pile	2360	980	1247	1030	2410
B.M (kN.m) in pier	6460	16020	15670	21960	6670

6.6. Influence of vertical soil resistance (t-z springs)

6.6.1. On pile

The envelope of axial force, shear force and bending moment in pile is shown in Figss. 25–28 with the effect of lateral soil resistance (p-y springs) as well as vertical soil resistance (t-z springs) for Imperial earthquake. These envelope are shown only for the proposed rocking bridge. It can be seen that shear force and bending moment are not affected when the vertical soil resistance is removed. However, there is a small increase in axial force in piles when only lateral soil resistance is modelled. When t-z springs are added to the system some share of axial force (which depends on soil properties) is contributed by the soil and hence axial force in pile is reduced.

6.6.2. On pier

The influence of vertical soil resistance (t-z springs) has also been studied on the pier of the rocking bridge only. As expected and shown in Figs. 29–32 that the pier forces and moment has little effect on the soil resistance modelled in lateral and vertical direction of piles.

6.7. Comparison of moment rotation curves

The moment rotation loops are shown in Fig. 33 for the conventional bridge and rocking bridge for the piers P1, P2 and P3. It can be observed that the loops of the rocking bridge have smaller area than the existing conventional bridge. This is an indication that a smaller pier size is possible for the rocking bridge piers. The pinch shape loops of the rocking bridge piers that are almost passing through the origin is an indication of the self-centering ability of the system and negligible residual deformation after an earthquake.

6.8. Comparison of ductility demands for the pier models

The comparison of average ductility demand (μc) of the rocking bridge piers and the conventional bridge piers are shown in Tables 15 and 16 respectively. The rocking bridge piers are approximately twice more ductile than the conventional bridge pier except those at abutment ends. Thus, uniform distribution of ductility demand is achieved at piers P1, P2 and P3 of rocking bridge as seen in Fig. 34.

6.9. Stresses in elastomeric pads

The maximum and minimum vertical stress in pads under each pier of rocking bridge for all the seven time histories is shown in Table 17. The average of maximum stress in pad is 7.24 MPa under pier P1 as it supports a larger span than the other piers. This stress is within the permissible limit of Eurocode [22] which restricts the limit of vertical stress to 25 MPa. Thus, the size of bearing chosen for the rocking bridge is safe as it was designed considering the parameter mentioned in design of elastomeric pads as per European practice.

6.10. Footing uplift

The Fig. 35 shows the uplift of footing at left node, central node and the right node of corners of the footing below the pier. It has been observed that the contact of footing is not lost with the pads placed below the footing and the chosen configuration does not allow uplift of footing. The maximum vertical compression which is found in pads below footing of pier P1 is 17.9 mm due to large span of superstructure supported at pier P1. The abutment pier (A1 and A2) supports lesser span and thus the pad is subjected to lesser vertical compression.

6.11. Comparison of pushover curves

The Fig. 36 shows the results of displacement controlled non-linear static pushover analysis of both the bridges in longitudinal direction only. The displacment is applied at deck level and the control point is where the displacments are monitored which is the position of the maximum displacment of the superstructure [27]. In both the bridges considered, the maximum displacment is at the abutment ends where longitudinally sliding bearings are provided only in the existing bridge. The rocking bridge is subjected to high lateral resistance as the stoppers prevent the complete failure of system and thus the pushover curve does not show any loss of strength. From the pushover curves,it has been also found that the ductility capacity (ratio of maximum displacement to the yield dispalacment) of rocking bridge is very high than

Table 10
Average of the maximum values of the seismic loading for PGA 0.30 g (Rocking Bridge).

Parameter	PGA 0.3 g (Rocking Bridge)				
	Pier A1	Pier P1	Pier P2	Pier P3	Pier A2
Horizontal movement at pier top (mm)	2.7	2.057	3.014	5.343	6.457
Residual Drift (%)	0.03	0.021	0.035	0.071	0.088
Axial force (kN) in pier (max/min)	−5917/-5718	−13686/-13229	−12405/-12069	−7572/-7466	−4184/-3789
Axial force (kN) in piles (max/min)	−1947/-1617	−3037/-1899	−2876/-1714	−2844/-1736	−1537/-1157
Shear force (kN) in pier	1379	3772	692	1763	1508
Shear force (kN) in piles	407	182	180	185	393
B.M (kN.m) in pile	2065	937	937	952	2057
B.M (kN.m) in pier	5659	16058	3625	8993	4824

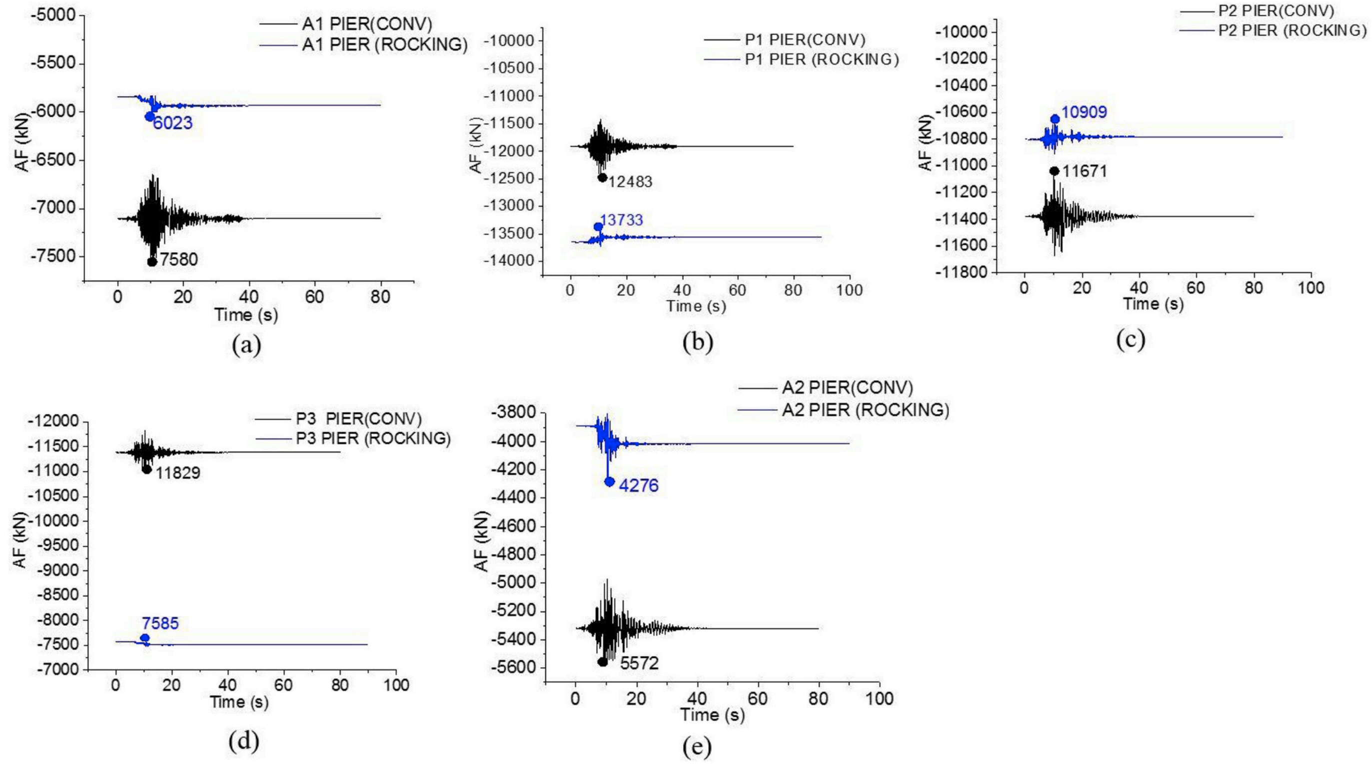

Fig. 21. Time history comparison of pier axial force for conventional bridge and the proposed rocking bridge for Imperial earthquake of PGA 0.6 g (a) Pier A1 (b) Pier P1 (c) Pier P2 (d) Pier P3 (e) Pier A2.

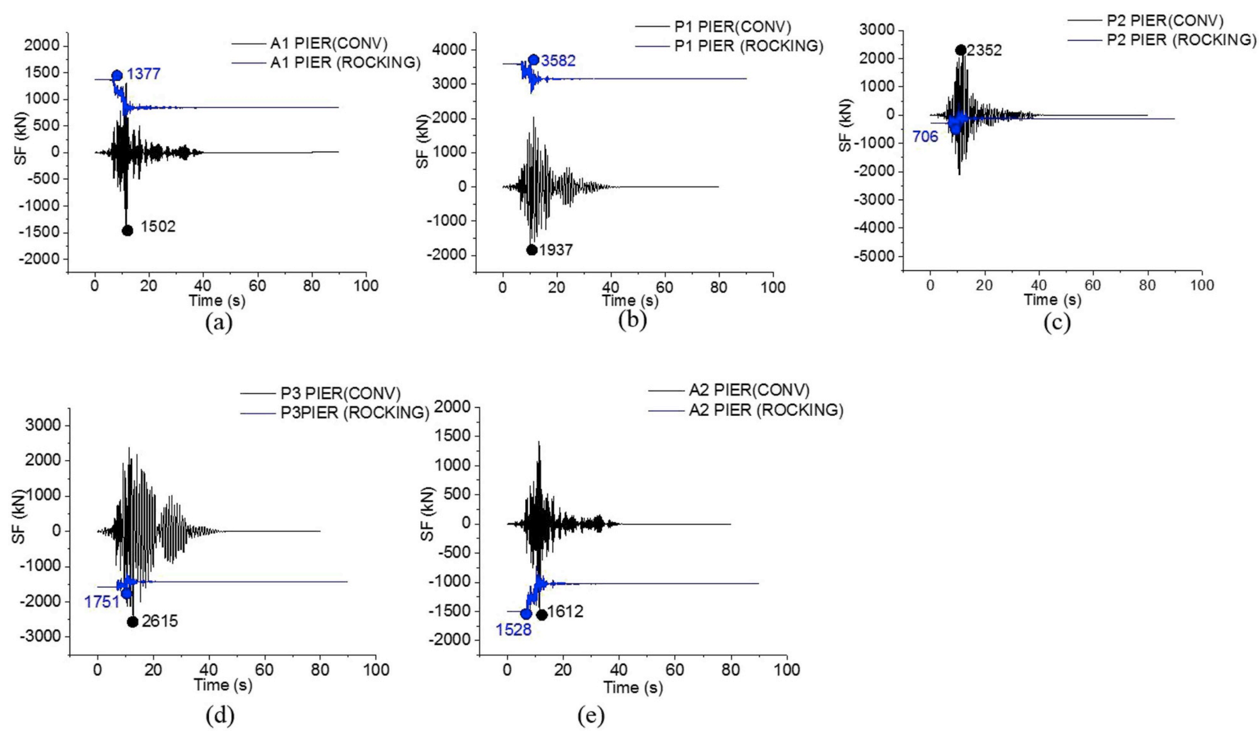

Fig. 22. Time history comparison of pier shear force for conventional bridge and the proposed rocking bridge for Imperial earthquake of PGA 0.6 g (a) Pier A1 (b) Pier P1 (c) Pier P2 (d) Pier P3 (e) Pier A2.

that of the existing conventional system as in rocking bridge the slight non-linearity is reverisble provided the footing ends of pier and the stopper are well protected. It can be also noted from these curves that the complete failure of the existing system (where base shear is zero) occur at 65 mm for the conventional bridge adopted in the current practice of bridge design.

6.12. Comparison of accleration displacement response spectra (ADRS)

The ADRS plot aims at evaluating the seismic performance point

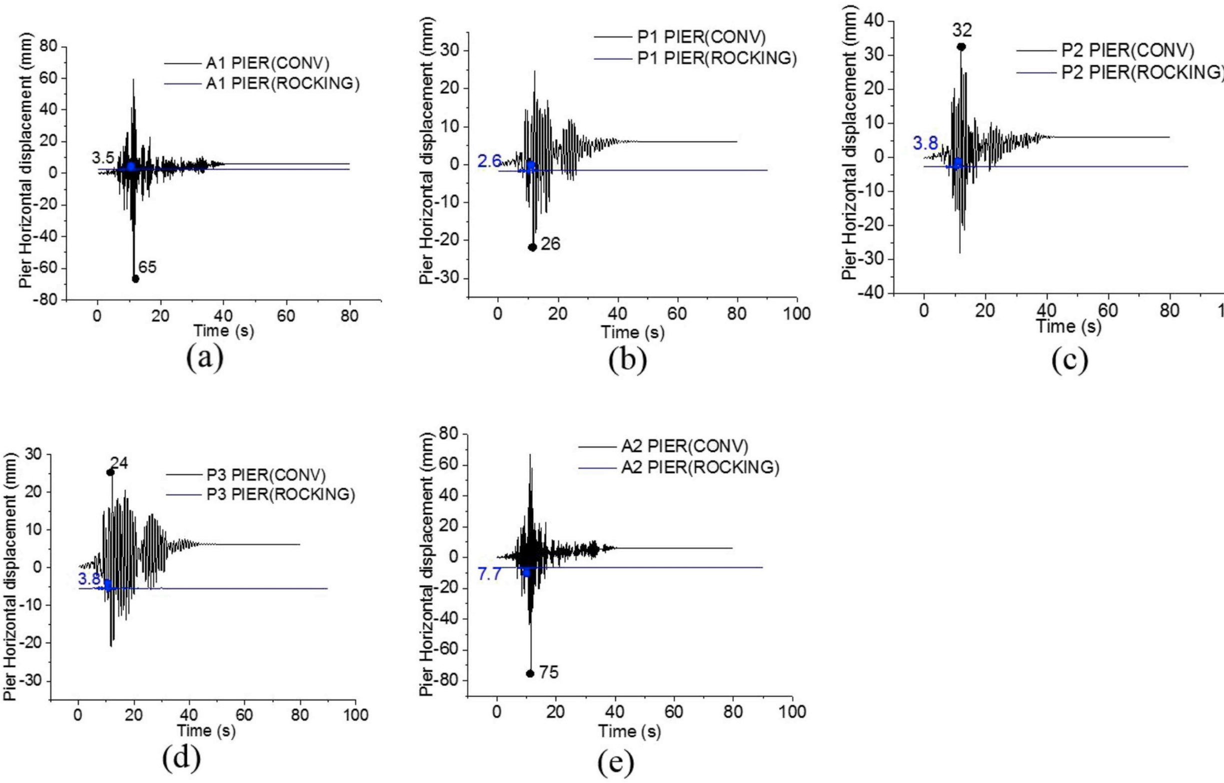

Fig. 23. Time history comparison of pier horizontal displacement for conventional bridge and the proposed rocking bridge for Imperial earthquake of PGA 0.6 g (a) Pier A1 (b) Pier P1 (c) Pier P2 (d) Pier P3 (e) Pier A2.

Table 11
Residual drift(%) of existing bridge for seven time histories.

EQ	Residual drift (%) of Existing Bridge				
	Pier A1	Pier P1	Pier P2	Pier P3	Pier A1
	h = 7.7 m	h = 7.7 m	h = 7.7 m	h = 7.7 m	h = 7.7 m
Imperial	0.051	0.069	0.060	0.110	0.090
Chi-Chi	0.117	0.095	0.032	0.068	0.039
Hollister	0.065	0.083	0.063	0.124	0.104
Kocaeli	0.026	0.092	0.029	0.066	0.012
Kozani	0.10	0.166	0.104	0.132	0.061
Loma Prieta	0.018	0.084	0.021	0.058	0.020
Northridge	0.063	0.130	0.067	0.095	0.025
Mean	0.063	0.103	0.054	0.093	0.050

Table 12
Residual drift(%) of rocking bridge for seven time histories.

EQ	Residual drift (%) of Rocking Bridge				
	Pier A1	Pier P1	Pier P2	Pier P3	Pier A1
	h = 7.7 m	h = 7.7 m	h = 7.7 m	h = 7.7 m	h = 7.7 m
Imperial	0.031	0.020	0.034	0.070	0.087
Chi-Chi	0.029	0.022	0.036	0.071	0.088
Hollister	0.029	0.021	0.036	0.071	0.088
Kocaeli	0.030	0.021	0.035	0.071	0.088
Kozani	0.030	0.021	0.035	0.071	0.088
Loma Prieta	0.030	0.020	0.035	0.071	0.087
Northridge	0.029	0.021	0.036	0.071	0.088
Mean	0.030	0.021	0.035	0.071	0.088

Table 13
Maximum drift(%) of existing bridge for seven time histories.

EQ	Residual drift (%) of Existing Bridge				
	Pier A1	Pier P1	Pier P2	Pier P3	Pier A1
	h = 7.7 m	h = 7.7 m	h = 7.7 m	h = 7.7 m	h = 7.7 m
Imperial	0.844	0.338	0.416	0.338	0.974
Chi-Chi	0.305	0.130	0.169	0.143	0.312
Hollister	0.494	0.223	0.238	0.260	0.545
Kocaeli	0.377	0.166	0.208	0.182	0.429
Kozani	0.571	0.208	0.216	0.247	0.631
Loma Prieta	0.519	0.234	0.286	0.221	0.545
Northridge	0.442	0.312	0.247	0.338	0.390
Mean	0.507	0.230	0.254	0.247	0.547

Table 14
Maximum drift(%) of rocking bridge for seven time histories.

EQ	Residual drift (%) of Rocking Bridge				
	Pier A1	Pier P1	Pier P2	Pier P3	Pier A1
	h = 7.7 m	h = 7.7 m	h = 7.7 m	h = 7.7 m	h = 7.7 m
Imperial	0.045	0.034	0.049	0.084	0.100
Chi-Chi	0.034	0.029	0.042	0.077	0.094
Hollister	0.038	0.027	0.043	0.078	0.095
Kocaeli	0.040	0.030	0.044	0.079	0.096
Kozani	0.042	0.032	0.047	0.082	0.099
Loma Prieta	0.048	0.036	0.051	0.086	0.104
Northridge	0.044	0.032	0.048	0.084	0.100
Mean	0.042	0.031	0.046	0.081	0.098

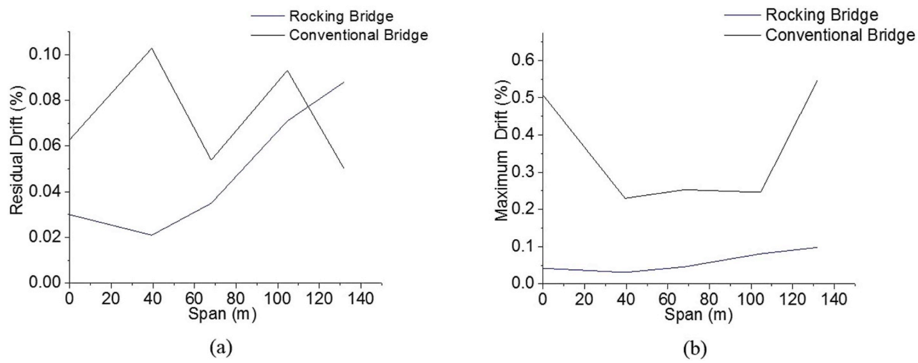

Fig. 24. (a) Average residual drift variation at pier along span (b) Average maximum drift variation at pier along span.

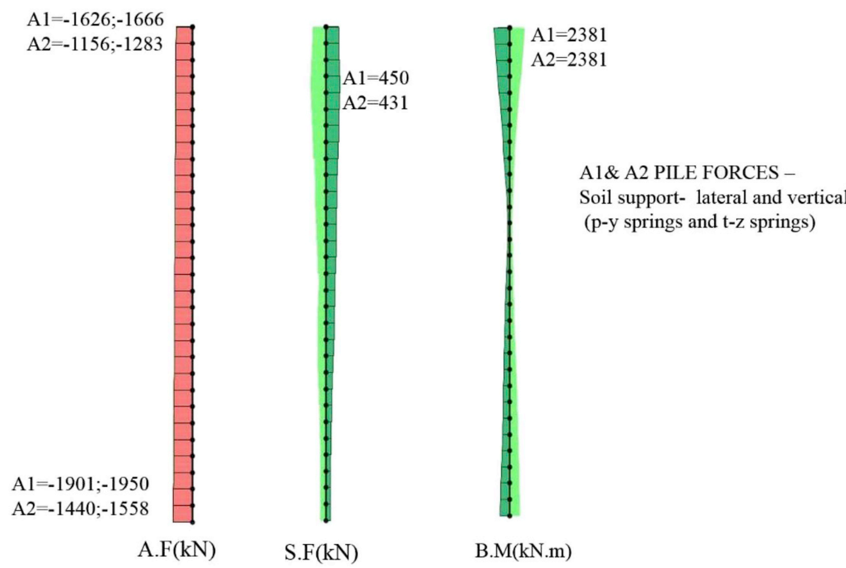

Fig. 25. Envelope of pile forces at A1 and A2 (Axial, Shear and Bending) for Imperial Earthquake with p-y and t-z springs.

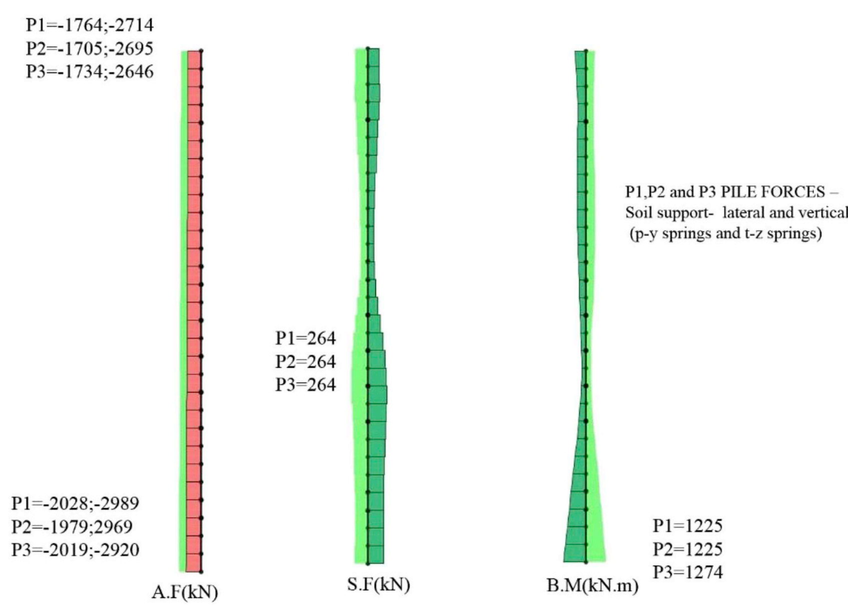

Fig. 26. Envelope of pile forces at P1,P2 and P3 (Axial, Shear and Bending) for Imperial Earthquake with p-y and t-z springs.

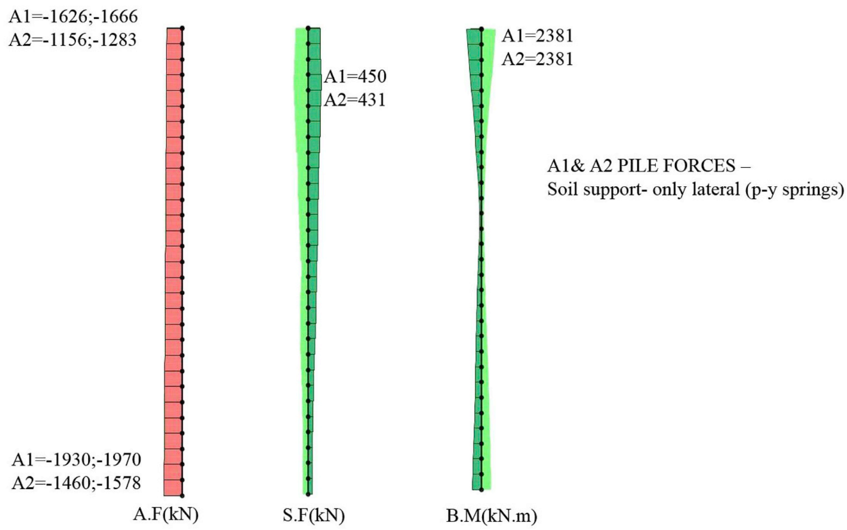

Fig. 27. Envelope of pile forces at A1 and A2 (Axial, Shear and Bending) for Imperial Earthquake with only p-y springs.

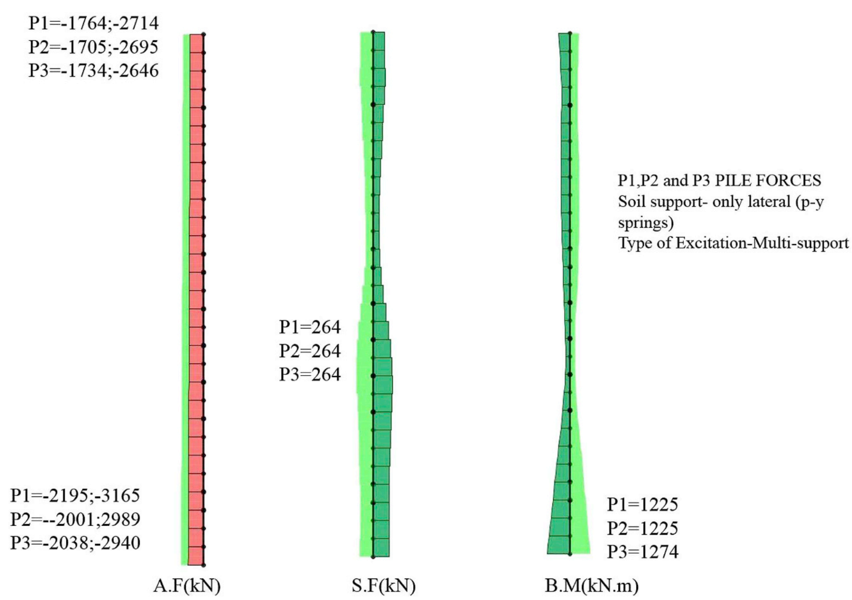

Fig. 28. Envelope of pile forces at P1,P2 and P3 (Axial, Shear and Bending) for Imperial Earthquake with only p-y springs.

where the capacity of the structure matches the demand during an earthquake.If the performance point occurs within the central portion of the capacity curve or closer to the point where elastic range of structure ends then it is an indication that the structure would suffer less damage during an earthquake [28]. The site seismic coefficients Ca and Cv are both 0.3 and structural behaviour type B (which are in close approximation of the existing site) was chosen to plot the accleration displacement response spectra. The increase spectral accleration as seen in case of rocking bridge is an indication that the capacity to survive in servere earthqukaes Also, as seen in Fig. 37 the spectral displacement of rocking bridge is twice less than the conventional one as the rocking bridge has integral superstructure at all the pier ends and the similar reduction in pier displacement was also observed from the THA analysis performed.

7. Conclusions

This paper proposes a novel rocking resilient pier foundation which uses elastomeric pads at the base of footing supported on pile foundation. The proposed rocking bridge has been compared with the existing rail over bridge which has conventional system of superstructure being simply supported on pier cap. The basis of comparison are displacements, drifts and forces in piers. Only horizontal seismic excitation in the longitudinal direction of bridge is considered in this study. Based on the analysis performed the following conclusions were drawn:

1. The proposed rocking pier bridge on elastomeric pads on pile foundation is subjected to less bending moment in pier as compared to the conventional rail over bridge considered in this study. Also, the pier bending moments of the proposed bridge remained in elastic range as the moments were below the yield moments. The pile moments in the rocking bridge are also decreased by approximately 12–15% when compared to the target bridge.

2. The superstructure of the rocking bridge is not subjected to any uplift as pier was in compression and had low axial fluctuations for the given arrangement of elastomeric pads placed beneath the footing of the pier.
3. The shear forces in the pier of proposed rocking bridge were approximately twice than that of the conventional bridge. Thus, for bridge with rocking pier the ties/stirrups shall require closer spacing

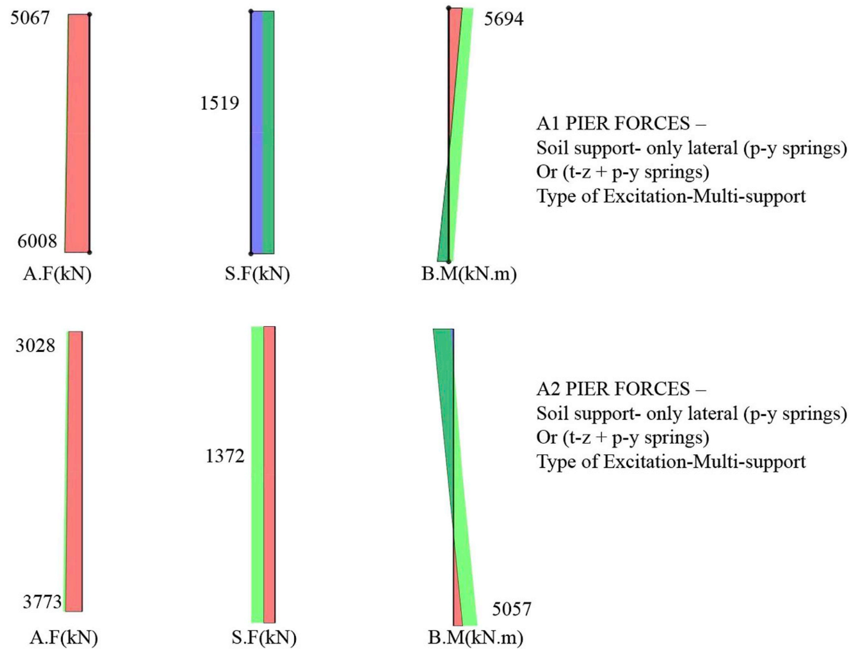

Fig. 29. Envelope of pier forces at A1 and A2 (Axial, Shear and Bending) for Imperial Earthquake.

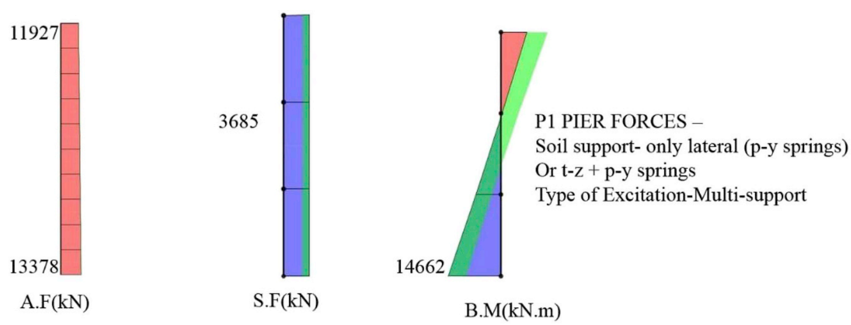

Fig. 30. Envelope of pier forces at P1 (Axial, Shear and Bending) for Imperial Earthquake.

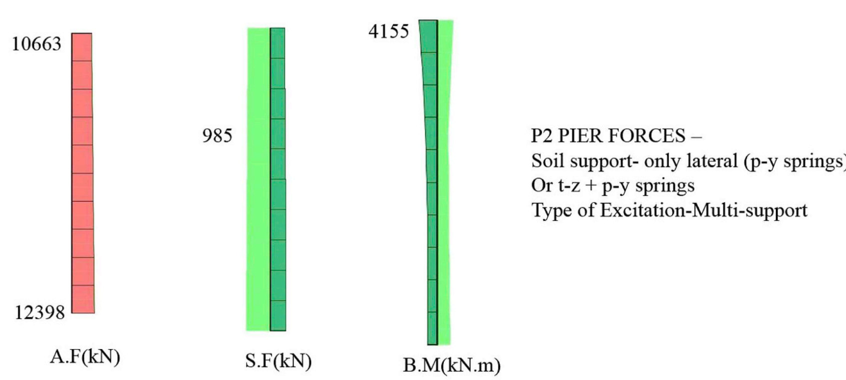

Fig. 31. Envelope of pier forces at P2 (Axial, Shear and Bending) for Imperial Earthquake.

and better confinement in the pier section as compared to the fixed base piers.

4. The rocking pier bridge had negligible residual drifts which was also shown by the moment rotation curves which were almost passing through the axis of origin which is good indication of self-centering capacity of the rocking bridge system. Thus, the rocking bridge has enhanced post-earthquake serviceability.
5. The distribution of ductility demand was uniform in the rocking bridge and the piers of the same was twice more ductile than the conventional pier adopted in current practice of bridge substructure design.
6. The proposed rocking bridge has better seismic performance than the conventional one as seen from ADRS plot where the rocking bridge has ability to sustain large earthquakes due to the increased

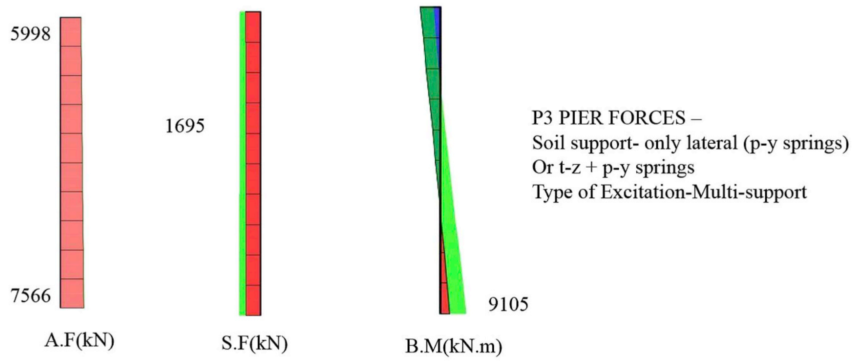

Fig. 32. Envelope of pier forces at P3 (Axial, Shear and Bending) for Imperial Earthquake.

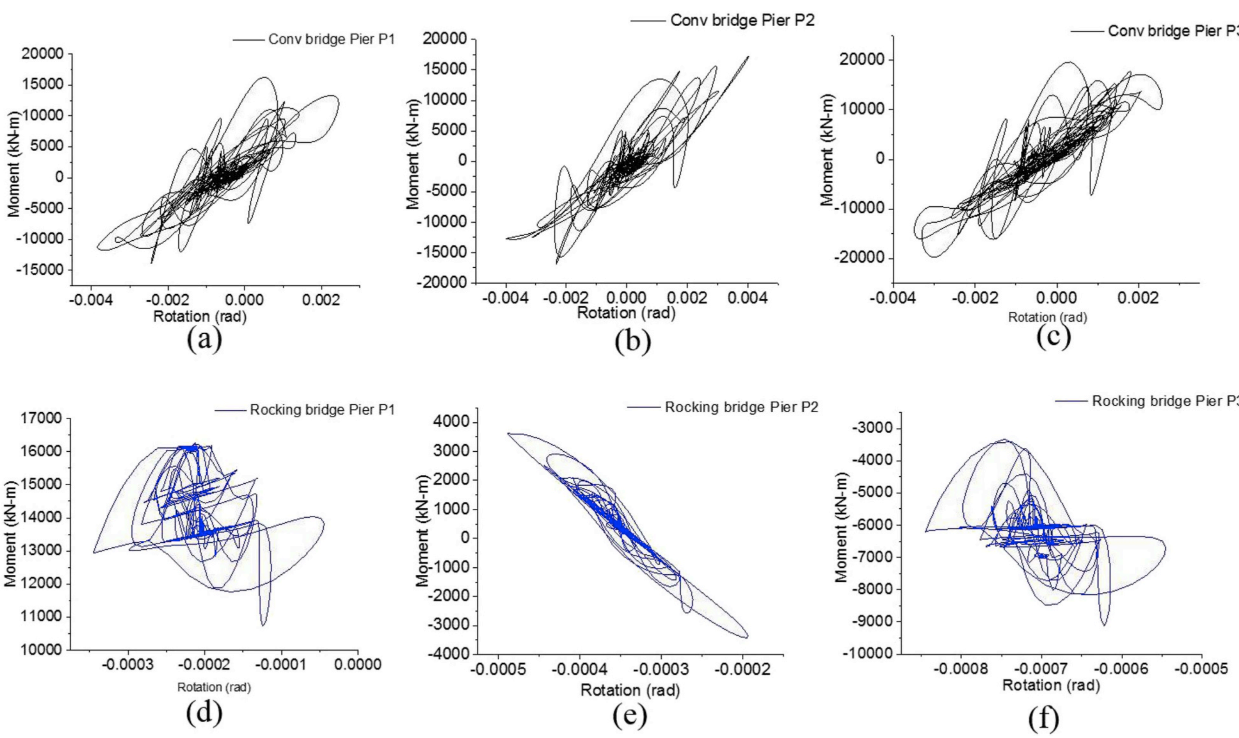

Fig. 33. Comparison of moment rotation response for Imperial Earthquake 0.3 g (a) Conv Pier P1 (b) Conv Pier P2 (c) Conv PierP3 (d) Rocking Pier P1 (e) Rocking Pier P2 (f) Rocking Pier P3

Table 15
Average Ductility Demand at pier location of rocking bridge from non-linear time history analysis.

Parameter	Pier A1	Pier P1	Pier P2	Pier P3	Pier A2
Peak Drift (%)	0.042	0.031	0.046	0.081	0.098
Yield Drift (%)	0.007	0.0216	0.0129	0.0127	0.027
Ductility Demand,μd	5.4	1.4	1.3	1.2	3.5

Table 16
Average Ductility Demand at pier location of conventional bridge from non-linear time history analysis.

Parameter	Pier A1	Pier P1	Pier P2	Pier P3	Pier A2
Peak Drift (%)	0.49	0.29	0.27	0.29	0.53
Yield Drift (%)	0.52	0.53	0.53	0.45	0.57
Ductility Demand,μd	0.94	0.55	0.51	0.64	0.93

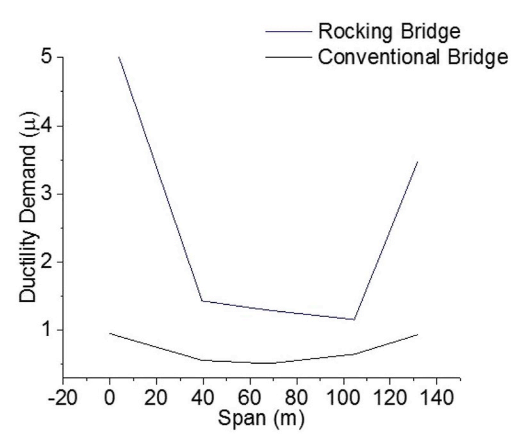

Fig. 34. Average pier ductility demand for THA.

Table 17
Maximum and Minimum stresses in pad of the Rocking Bridge.

EQ	Stresses(MPa) in Pad under each piers					
	Pier P1		Pier P2		Pier P3	
	Max	Min	Max	Min	Max	Min
Imperial	7.25	5.39	6.41	5.57	6.48	4.88
Chi-Chi	6.99	5.71	6.29	5.69	6.16	5
Hollister	7.26	5.68	6.37	5.64	6.21	4.81
Kocaeli	7.12	5.73	6.34	5.71	6.25	4.94
Kozani	7.3	5.82	6.35	5.65	6.28	4.79
Loma Prieta	7.36	5.4	6.47	5.52	6.56	4.99
Northridge	7.42	5.39	6.45	5.55	6.29	4.61
Mean	7.24	5.59	6.38	5.62	6.32	4.86

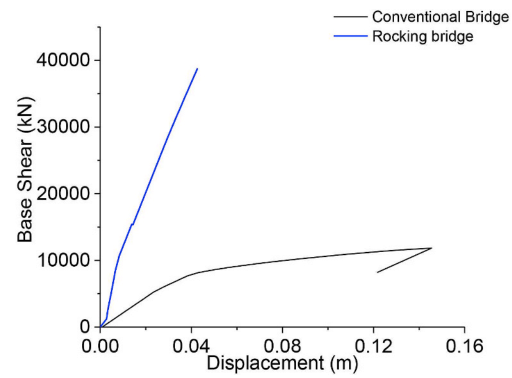

Fig. 36. Pushover curve comparison at pier P1 of rocking bridge and the existing conventional bridge.

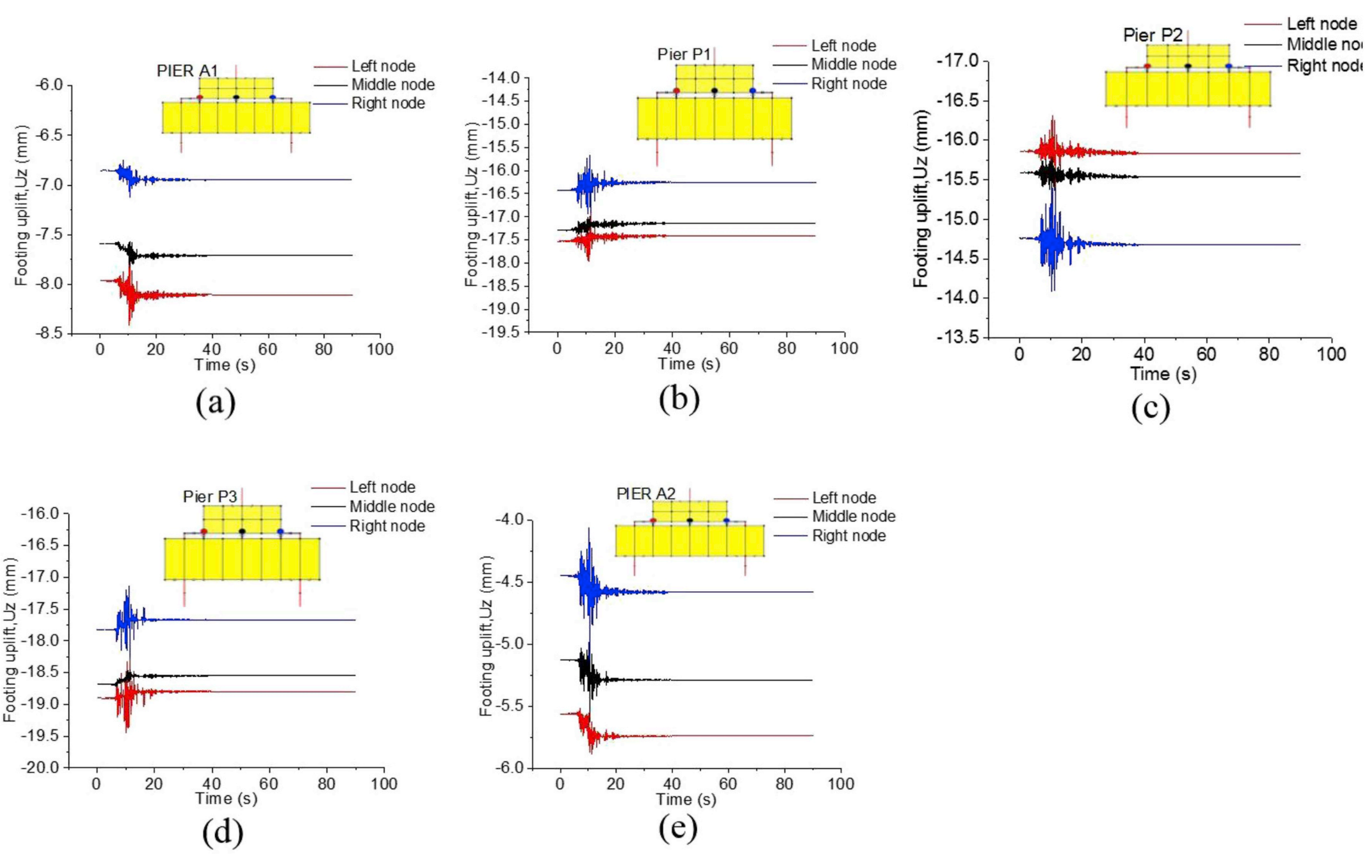

Fig. 35. Time history of footing uplift for rocking bridge for Imperial Earthquake 0.3 g (a) P1 pier (b) P2 pier (c) P3 pier.

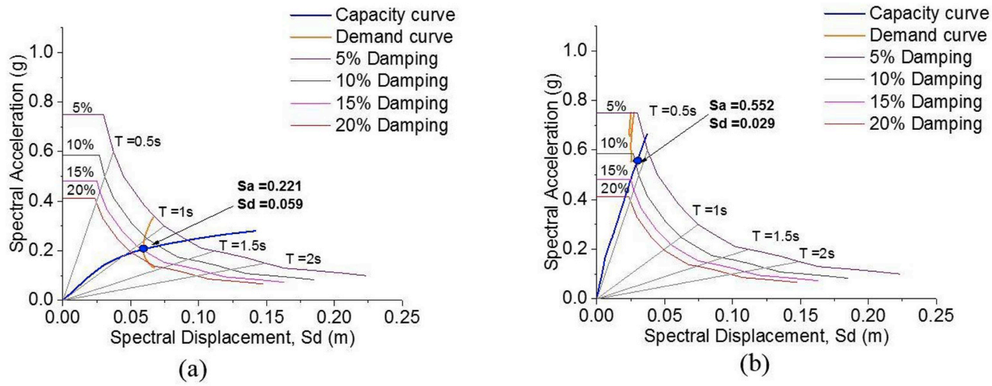

Fig. 37. Accleration Displacement Response Spectra (ADRS) (a) Existing conventional bridge (b) Proposed rocking bridge.

spectral acceleration than the conventional bridge. Also, the fundamental period of vribration was enhanced which makes rocking bridge more flexible than the conventional bridge.

Acknowledgements

The continuous support and assistance provided by bridge design firm, *R.R Consulting Engineers* (India), for the existing bridge considered in this research study is highly appreciated by the first author. The initial guidance on the concept of rocking structures on pads with spread foundations was provided by Professor George Mylonakis (University of Bristol, UK) is highly valued and greatly appreciated by the authors.

Appendix A. Supplementary data

Supplementary data to this article can be found online at https://doi.org/10.1016/j.soildyn.2019.05.018.

Appendix

The following figures (Fig A1 and Fig A2) give details of pier and pile cross-section along with reinforcement details of the existing bridge and the same is adopted for the proposed bridge for comparative study. The superstructure cross-section of the exsiting bridge is also shown in Fig. A3.

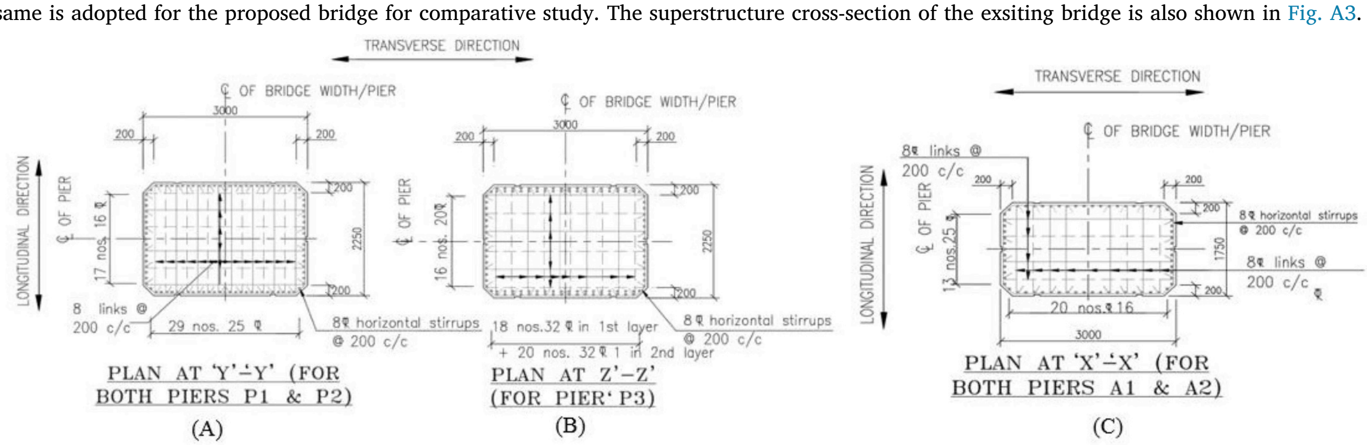

Fig. A.1. (a) Cross-section for pier P1 & P2 with steel ratio, $\rho_l = A_s/A_c = 0.52\%$. (b) Cross-section for pier P3 with steel ratio, $\rho_l = A_s/A_c = 1.0\%$. (c)Cross-section for pier A1 & A2with steel ratio, $\rho_l = A_s/A_c = 0.4\%$.

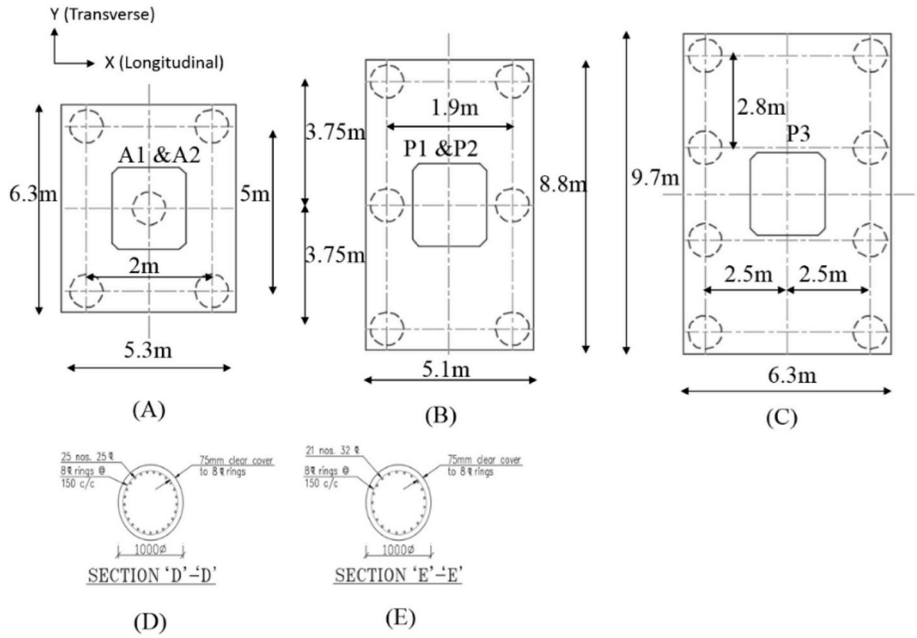

Fig. A.2. Pile configuration for (a) abutment pier A1 &A2 (b) pier P1 &P2 (c) pier P3 (d)Cross-section for pile A1, A2, P1& P 2 with steel ratio, $\rho_l = A_s/A_c = 1.56\%$. (e) Cross-section for pile P3 with steel ratio, $\rho_l = A_s/A_c = 2.15\%$2

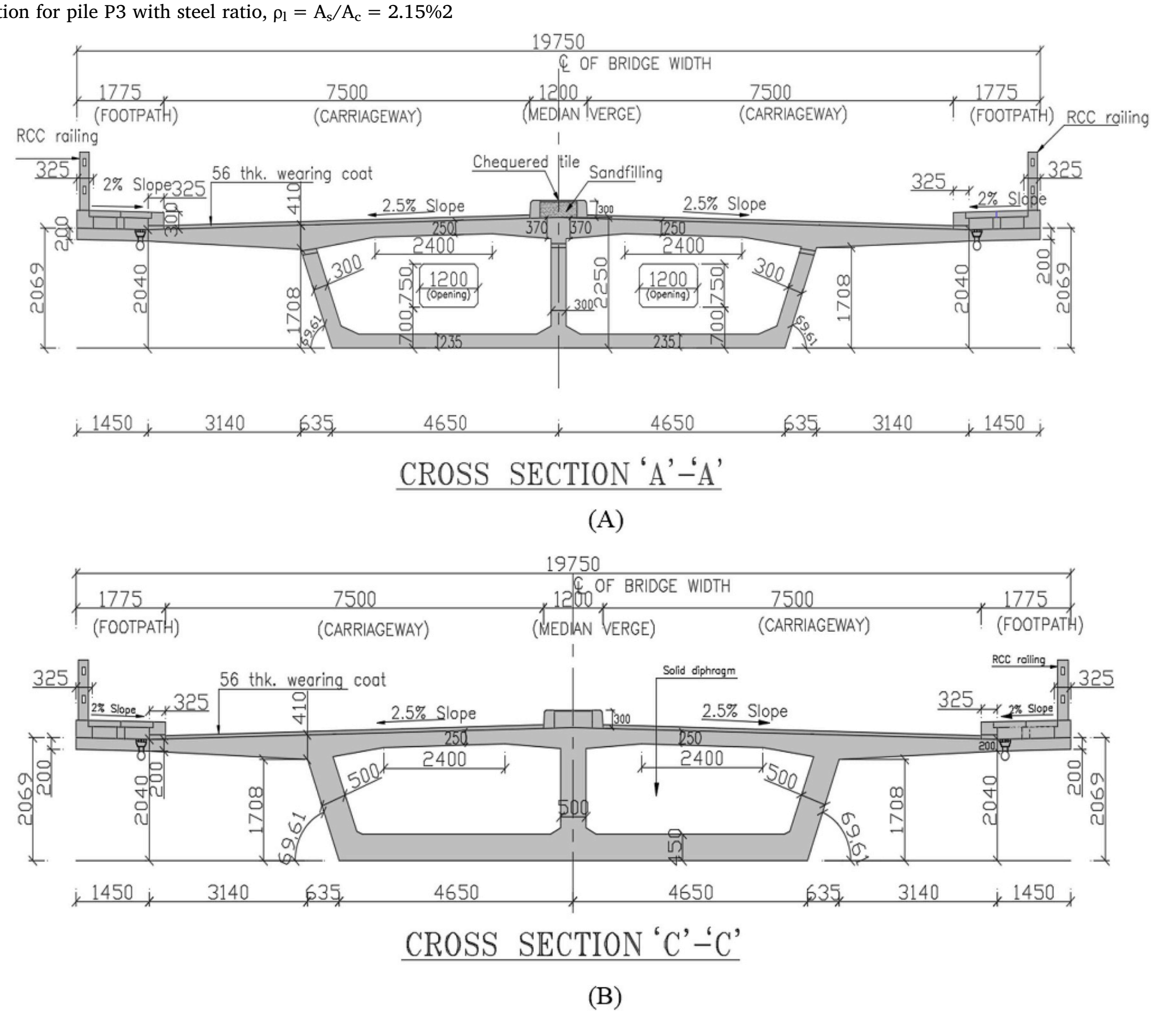

Fig A.3. Superstructure cross-section for both bridges (a) at Mid span (b) at Support3

References

[1] Åkesson B. Understanding bridge collapses. London, UK: Taylor & Francis; 2008.
[2] Priestley M, Seible F, Calvi G. Seismic design and retrofit of bridges. New York: Wiley; 1996.
[3] Makris N, Vassiliou. The dynamics of the rocking frame. Seismic assessment, behavior and retrofit of heritage building and mouments. Comput Methods Appl Sci 2015. https://doi.org/10.1007/978-3-319-16130-3.
[4] Anastasopoulos I, Loli M, Georgarakos T, Drosos V. Shaking table testing of rocking-isolated pier on sand. J Earthq Eng 2013;17:1–32.
[5] Palermo A, Mashal M. Acclerated bridge construction and seismic damage resistant technology: a New Zealand challange. Bull N Z Soc Earthq Eng 2012;45(3):123–34.
[6] Liu R, Palermo A. Low damage design and seismic isolation: what's the difference? New Zealand society for earthquake engineering conference. 2015.
[7] Antonellis G, Panagiotou M. Seismic Response of Bridges with rocking foundations compared to fixed-base bridges at a near fault site. J Bridge Eng 2014;19(15):1–14. ASCE.
[8] Jacquelyn DA, Kutter BL. Design Considerations for rocking foundations on unattached piles. J Geotech Geo Environ Eng 2014;10:1–11. 1061/(ASCE) GT.1943-56065.000162.
[9] Silva FD, Manzari TM. Seismic evaluation of pile foundation systems subjected to rocking. *12th world Conference on earthquake engineering.* 2012. [Lisboa].
[10] Quinn HB, Civjan SA. Parametric study on effects of pile orientation integral abutment bridges. J Bridge Eng 2015;9(13):1–16. ASCE.
11 Boulanger R,W, Curras JC, Kutter BL, Wilson D,W, Abghari A. Seismic soil-pile-structure interaction experiments and analysis. J Geotech Geo environ Eng 1999;125(9):750–9.
[12] Agalianos A, Psychari A, Vassiliou MF, Stojadinovic B, Anastasopoulos I. Comparative assessment of two rocking isolation techniques for a motorway overpass bridge. Front Built Environ 2017. https://doi.org/10.3389/fbuilt.2017.00047.
[13] IRC: 6"Standard specifications and codes of practice for road bridges, Section-II-Loads and Load combinations. New Delhi, India: Indian Road Congress (IRC); 2017.
[14] IRC: 78"Standard specifications and codes of practice for road bridges, Section-VII Foundation and substructure. New Delhi: Indian Road Congress (IRC); 2014.
[15] IRC: 112"Code of practice for concrete bridges 2011, New Delhi, India.
[16] Freyssinet flat jacks brochure. 2016. [France].
[17] Computers and Structures, Inc. CSI analysis and reference manual for CSI BRIDGE. CA: Computers and Structures, Inc. Berkeley; 2018.
[18] Caltrans Bridge design specifications manual. California Department of Transportation; 1990.
[19] Mander J, Priestley M, Park R. Theoretical stress-strain model for confined concrete. J Struct Eng 1988:1804–26. 10.1061/(ASCE)0733-9445(1988)114:8(1804).
[20] Wen YK. Method for random vibration of hysteretic systems ASCE J *Eng Mech Div* 1976;102. N0.EM2.
[21] Nagarajaiah S, Reinhorn AM, Constantinou MC. *3D-Basis:Nonlinear dynamic Analysis of three-dimensiona; base isolated structures:Part II* ,techincal repeort NCEER91-0005,national center for earthquake engineering research. Buffalo, N.Y: State University of New York at Buffalo; 1991.
[22] BSI (British Standards Institution). Structural Bearings. Part 3—Elastomeric Bearings. 2005. EN 1337-3, London.
[23] Naeim F, Kelly JM. Design of seismic isolated structures: from Theory to Practice. New York: Wiley; 1999.
[24] API (AmericanPetroleum Institute). Recommended practice for planning, designing and construction fixed offshore platforms-Working stress design. 1993. [Washington, DC].
[25] BSI (British Standards Institution). Eurocode 8: design of structures for earthquake resistance–Part 2: bridges BS EN 1998-2 2005. [London].
[26] Hashash YMA, Musgrove MI, Harmon JA, Groholsk DR, Phillips CA, Park D. DEEPSOIL version 7.0. 2017. [User Manual].
[27] Kappos AJ, Saiidi MS, Aydinoglu MN, Isakovic T. Seismic design and assessment of bridges. Dordrecht: Springer Science + Business Media; 2012. [Netherlands].
[28] Applied Technolgy Council (ATC). Report No. ATC 40 Seismic evalustion and retrofit of concrete buldings vol. 1. 1996. [RedwoodCity ,CA].
[29] Dammala PK, Krishna AM, Bhattacharya S, Nikitas G, Rouholamin M. Dynamic soil properties for seismic ground response studies in Northeastern India. J Soil Dyn Earthq Eng 2017;99:157–67.
[30] Yoshida N. Seismic ground response analysis. first ed. London: Springer; 2015.
[31] Guan Z, Chen Xu, Li J. Experimental investigation of the seismic performance of bridge models with conventional and rocking pile group foundations. Eng Struct 2018;168:889–902.